Asian Journal of Atmospheric Environment
Vol. 4-3, pp.115-140, December 2010

Characterization of Individual Atmospheric Aerosols Using Quantitative Energy Dispersive-Electron Probe X-ray Microanalysis: A Review

HyeKyeong Kim and Chul-Un Ro*

Department of Chemistry, Inha University, Incheon 402-751, Korea

*Corresponding author. Tel: +82-32-860-7676, E-mail: curo@inha.ac.kr

ABSTRACT

Great concerns about atmospheric aerosols are attributed to their multiple roles to atmospheric processes. For example, atmospheric aerosols influence global climate, directly by scattering or absorbing solar radiations and indirectly by serving as cloud condensation nuclei. They also have a significant impact on human health and visibility. Many of these effects depend on the size and composition of atmospheric aerosols, and thus detailed information on the physicochemical properties and the distribution of airborne particles is critical to accurately predict their impact on the Earth's climate as well as human health. A single particle analysis technique, named low-*Z* particle electron probe X-ray microanalysis (low-*Z* particle EPMA) that can determine the concentration of low-*Z* elements such as carbon, nitrogen and oxygen in a microscopic volume has been developed. The capability of quantitative analysis of low-*Z* elements in individual particle allows the characterization of especially important atmospheric particles such as sulfates, nitrates, ammonium, and carbonaceous particles. Furthermore, the diversity and the complicated heterogeneity of atmospheric particles in chemical compositions can be investigated in detail. In this review, the development and methodology of low-*Z* particle EPMA for the analysis of atmospheric aerosols are introduced. Also, its typical applications for the characterization of various atmospheric particles, i.e., on the chemical compositions, morphologies, the size segregated distributions, and the origins of Asian dust, urban aerosols, indoor aerosols in underground subway station, and Arctic aerosols, are illustrated.

Key words: Low-*Z* particle EPMA, Single particle analysis, Asian Dust, Urban aerosol, Subway particle, Arctic aerosol

1. INTRODUCTION

Atmospheric aerosols encompass a wide range of compositions and sizes that depend on their origins. A large fraction of aerosols, such as soil dust and sea salt particles, are natural in origin. Whereas anthropogenic aerosols, such as secondary sulfates, nitrates, organics, and soot, originate from urban and industrial emissions and combustion processes. Great concerns about atmospheric aerosols are attributed to their multiple roles to atmospheric processes. For example, atmospheric aerosols influence global climate, directly by scattering or absorbing solar radiations and indirectly by serving as cloud condensation nuclei (Satheesh and Moorthy, 2005). They can also have a significant impact on human health and visibility. These effects depend on the size and composition of atmospheric aerosols, and thus detailed information on the physicochemical properties and the distribution of airborne particles is critical to reduce the uncertainty in the estimation of their impact on the Earth's climate and also for the control of the air quality.

Aerosol loading in the atmosphere is usually quantified by mass concentration, and bulk analysis has been generally utilized to characterize atmospheric particles. In bulk analysis, all particulate matters collected on a filter are handled as a single sample. As a result, the analytical data provide the average composition of the collected particles. However, as atmospheric particle samples are heterogeneous mixture of various forms of chemical compounds, the average composition is not sufficient to reveal the diversity of the particles in the sample. In addition, airborne aerosols independently move and react in the air. Therefore, advanced single particle micro-analytical techniques capable of providing detailed information on chemical, microphysical, and optical properties on a micrometer scale are required in order to describe the chemical micro-processes in (or on) aerosol particles

(Frustorfer and Niessner, 1994).

The two most popular types of single particle analytical techniques are (i) aerosol time-of-flight mass spectrometry (ATOFMS) and (ii) energy dispersive electron probe X-ray microanalysis (ED-EPMA). ATOFMS can identify chemical species of individual particles qualitatively, using laser microprobe mass spectrometry (Carson *et al.*, 1997; Noble and Prather, 1996). The technique can analyze the aerodynamic sizes and chemical compositions of individual particles in real time and even the instrument can be portable (Gard *et al.*, 1997). By the application of the ATOFMS technique, the complex nature of airborne particles has been directly revealed (Murphy and Thomson, 1997a, b) and it was demonstrated that the technique can clearly elucidate the atmospheric chemistry between sea-salt particles and gas-phase nitric acid, as it occurs in the atmosphere (Gard *et al.*, 1998). However, due to its poor reproducibility, the technique can only provide qualitative determination of chemical species in individual particles.

ED-EPMA technique, employing a scanning electron microscope (SEM) equipped with an energy dispersive X-ray (EDX) detector, has been widely utilized for the characterization of minute solid samples. Electron images obtained from SEM provides information on micro-structures of samples and X-ray spectra obtained by EDX detector gives information on chemical compositions, and thus ED-EPMA has been used to characterize the chemical compositions and morphologies of individual airborne particles (Jambers and Van Grieken, 1997; Osán *et al.*, 1996). However, conventional ED-EPMA is not suitable for low-*Z* ($Z < 11$) element analysis since a Be window in front of conventional EDX detectors absorbs soft X-rays emitted from the low-*Z* elements. In 1999, was developed an improved method, denoted "low-*Z* particle EPMA", that can determine the concentration of low-*Z* elements such as carbon, nitrogen, and oxygen in a microscopic volume (Ro *et al.*, 1999). The capability of quantitative analysis of low-*Z* elements in individual particle allows the characterization of environmentally important atmospheric particles, such as sulfates, nitrates, ammonium salts, and carbonaceous particles. Furthermore, the diversity and the complicated heterogeneity of atmospheric particles in chemical compositions can be investigated in detail.

In this review, the development and methodology of low-*Z* particle EPMA technique for the characterization of atmospheric aerosols are introduced in sections 2 and 3, respectively. In section 4 of this review, are illustrated the size segregated distribution and their origins of various particle types in Asian dust, urban aerosols, indoor aerosols in a underground subway station, and Arctic aerosols, obtained by the application of low-*Z* particle EPMA.

2. DEVELOPMENT OF ED-EPMA FOR THE ANALYSIS OF ATMOSPHERIC PARTICLE

2.1 Thin-window/Windowless ED-EPMA

ED-EPMA is a powerful method for investigating the physicochemical properties of individual microscopic aerosols. However, conventional ED-EPMA has a limitation for the analysis of atmospheric aerosol particles given its limited capability for determination of low-*Z* elements such as carbon, nitrogen, and oxygen. This is a result of the Be window used for the protection of EDX detector, which absorbs the low-energy X-rays emitted from low-*Z* elements and subsequently hinders their detection. The ability of detection of low-*Z* elements in particulate matter allows enlarging the scope of single-particle analysis, firstly because the low-*Z* elements are abundantly present in environmental particles and secondly because quantitative information is necessary for the speciation of individual microscopic particles. Since sulfates, nitrates, and organics play a considerable part in atmospheric environment, the capability of detecting low-*Z* elements is inevitable for the analysis of atmospheric particles.

The feasibility of low-*Z* element analysis had been tried using thin-window and windowless EPMA. In 1992, Bishop *et al.* used ultra-thin window EDX detector for the analysis of sedimentary organic particles, and claimed the capability of qualitative assessment of the carbon, oxygen, sulfur, and chlorine contents in the particles. The first application of windowless EDX for single aerosol particles was reported by Hamilton *et al.* (1994). The authors were interested in the detection of airborne carbonaceous material, so the Whatman Anodisc alumina-based membrane filter was chosen as an appropriate filter material. Since the ceramic filter is non-conductive, gold sputtering was used. Due to the oxygen background of the alumina substrate and the additional absorption by the gold coating, the method was only suitable for the qualitative analysis of carbon. Frustorfer and Niessner (1994) tried to analyze atmospheric particles using conventional Nucleopore membrane filters as the sampling substrate. They applied silver coating on the sample (the X-ray peaks of Ag do not overlap with those of the elements of interest.) and tried to identify the sample particles by comparing X-ray spectra of various standard particles measured at the same instrumental conditions for the sample. The authors claimed that

the method identified soot particles as small as 50 nm in radius and their spectra could be distinguished from those of other particles or pure substrate in 500 ms live time measurements. However, the relatively high current (1-2 μA) at 25 kV might damage the submicron particles even within milliseconds.

These preliminary studies for the analysis of individual particles using thin window/windowless EDX could not derive even semi-quantitative results for the light elements. This is because of the fundamental problems to be solved. The first critical problem is that X-rays generated by low-*Z* elements are so soft (weak), therefore important matrix effects (mostly due to X-ray absorption) exist even in submicron particle. The second one is that the magnitude of matrix effects depends on the particle size and shape (geometric effect). Although low-*Z* elements can be detected by thin-window or windowless EDX detector, the matrix effect and the geometric effect in the microscopic volume must be solved to quantitatively analyze low-*Z* elements.

2. 2 Low-*Z* Particle EPMA

The popular correction methods for the quantitative EPMA are ZAF and $\phi(\rho z)$-based methods (Goldstein *et al.*, 2003). ZAR method includes atomic number effect (Z) and X-ray absorption correction (B), and X-ray fluorescence correction (F). $\phi(\rho z)$ is the X-ray depth distribution function which describes the distribution of X-ray generation beneath the surface. These methods are good for the samples having the flat surface and the homogeneous composition, that is, they exclude the geometric effects. Since aerosols are in various shapes, such as spherical or cubic, the consideration of geometric effect is essential for the quantitative analysis of atmospheric aerosols. In the past two decades, several research groups have dealt with the theoretical evaluation of the matrix and geometric effects for individual particles. A reliable and widely used quantification method for micro-particle analysis is so-called particle-ZAF algorithm developed by Armstrong and Buseck (1985). However, the particle-ZAF method based on the use of bulk standards introduces large errors for the analysis of light elements, mostly because of the large absorption correction for the low-*Z* elements and the difference in their behaviors between the bulk standard and single particles under electron bombardment. When the average atomic number of the substrate significantly differs from that of the particle, the side-scattering correction of the $\phi(\rho z)$ function is reasonable only if the electron excitation volume is smaller than the particle itself. Therefore, the $\phi(\rho z)$-based method is not suitable for the analysis of small particles (Armstrong, 1991).

Another quantification method is the standardless peak-to-background (P/B) method without using bulk standards (Lábár and Török, 1992). The method assumes that both characteristic and Bremsstrahlung background X-ray photons are emitted from the same region of the sample and experience the same absorption effect on their way to the detector. As it is assumed that the characteristic and background photons are generated within the particle, the method can only be used when the excitation volume is smaller than the particle volume. Also, the experimental determination of the background intensity at low photon energies is almost impossible when the spectral acquisition time is short. Therefore, only semi-quantitative analysis of relatively large particles ($D_p > 1$ μm) is feasible for the P/B method without the determination of low-*Z* elements.

The quantification of low-*Z* elements in ED-EPMA had been neglected until a methodology using a Monte Carlo calculation in an iterative approach was developed (Osán *et al.*, 2000; Szalóki *et al.*, 2000; Ro *et al.*, 1999). The Monte Carlo calculation with reverse iterative successive approximation, based on a modified version of the single scattering CASINO Monte Carlo program (Drouin *et al.*, 1997; Hovington *et al.*, 1997a, b), was reported to well describe the excitation interactions between electrons and the atoms of the matrix, and the matrix and geometric effects for fluorescence X-ray signals of low-*Z* elements in individual micro-particles (Ro *et al.*, 1999). The Monte Carlo calculation allows the simulation of electron trajectories in various shapes of particles, such as spherical, hemispherical, and hexahedral, sitting on a flat substrate. The simulation procedure also determines characteristic and Bremsstrahlung X-ray flux emitted from the particle and collecting substrate and the influence of the substrate material on the energy distribution of the exciting electrons. In the beginning of the iterative Monte Carlo calculation, the difference between the measured and the calculated (simulated) intensities is considerable so that a successive approximation approach is employed to find the better match between two intensity values, by adjusting input values, i.e., chemical compositions, in the following iteration. The iterative calculation stops when the measured X-ray intensities for all chemical elements in a particle are well matched to the simulated intensities by the Monte Carlo calculation. When convergence is achieved, the chemical composition of a particle can be obtained. Generally a few iterations are enough to find convergence.

When the Monte Carlo calculation was applied to various types of standard particles such as NaCl, SiO_2, $CaSO_4 \cdot 2H_2O$, $(NH_4)_2SO_4$, and NH_4NO_3, it

provided good results within 12% relative deviations between the calculated and nominal elemental concentrations (Ro *et al.*, 2003). The new method that can quantitatively analyze low-*Z* elements in microscopic volume was named as "low-*Z* particle EPMA" and has been widely used to characterize various types of ambient aerosol samples (Geng *et al.*, 2010, 2009a; Kang *et al.*, 2009, 2008; Hwang and Ro, 2006; Ro *et al.*, 2005, 2002, 2001a, b, 2000; Osán *et al.*, 2000).

3. METHODOLOGY OF LOW-*Z* PARTICLE EPMA TECHNIQUE

3. 1 Sampling Method

For the collection of size segregated aerosol particles, Dekati PM-10 and May cascade impactors were used. The 7-stage May cascade impactor has, at a 20 L/min sampling flow, aerodynamic cutoffs of 16, 8, 4, 2, 1, 0.5, and 0.25 μm for stages 1-7, respectively (May, 1975). The 3-stage Dekati PM-10 sampler has, at a 10 L/min sampling flow, aerodynamic cutoffs of 10, 2.5, 1 μm for stages 1-3, respectively. Silver or aluminum foil was used as the collection substrate. For the single particle analysis, particles should be placed on the substrate separately without agglomeration. Since the number concentration of the atmospheric particles increases with the decrease of particle size, it usually takes the shorter sampling time for the smaller particles. The collected samples were put in plastic carriers and stored in a desiccator before low-*Z* particle EPMA measurement.

3. 2 Measurements

Measurements were carried out on a Hitachi S-3500N SEM equipped with an Oxford Link SATW ultrathin window EDX detector. The resolution of the EDX detector is 133 eV for Mn K_α X-rays. X-ray spectra were recorded under the control of EMAX Hitachi software. To achieve optimal experimental conditions such as low level background in the spectra and the high sensitivity for light element analysis, a 10 kV accelerating voltage and 1.0 nA beam current were used for the measurements. In order to obtain statistically enough counts in the X-ray spectra and to minimize electron beam damage on particles, a typical measuring time of 10 s was used. The cold stage of the electron microscope allowed the analysis of particulate samples around $-193^{\circ}C$ using liquid nitrogen, which enabled us to minimize contamination and reduce beam damage to the samples as well. Computer-controlled X-ray data acquisition for individual particles was carried out automatically in the point analysis mode whereby the electron beam was focused at the center of each particle and X-rays were acquired while the beam remained fixed on this single spot. The localization of the particles was based on inverse backscattered electron contrast. Morphological parameters, such as diameter and shape factor, were calculated by using an image processing routine. These estimated geometrical data were used as input parameters for the Monte Carlo quantification procedure.

3. 3 Data Analysis

The net X-ray intensities for the elements were obtained by nonlinear least-squares fitting of the collected spectra using the AXIL program (Vekemans *et al.*, 1994), and the elemental concentrations of individual particles were obtained from their X-ray intensities by application of the Monte Carlo calculation with reverse successive approximations (Ro *et al.*, 2003). When elemental atomic concentrations of a particle are obtained as Ca ~20%: C ~20%: O ~60%, it indicates that the particle is composed of Ca, C, and O with the molar ratio of 1 : 1 : 3, which is a single component $CaCO_3$ particle. However, it is rare to find atmospheric particles composed of only a single chemical species due to the atmospheric physical mixing and chemical processing in the air. Since most atmospheric particles are found as mixtures of two or more chemical species, a systematic methodology is necessary for speciation of individual particles.

A methodology was employed to classify individual particles as follows. First, elements with less than 1.0% of atomic concentration were excluded in the procedure of chemical speciation, as ED-EPMA has high detection limits of 0.1-1.0 wt.% mainly due to its high Bremsstrahlung background level. Since sample particles have a microscopic volume (pg range in mass for a single particle of micrometer size), the elements at trace levels could not be reliably investigated. Second, if single chemical species with more than 90% in concentration comprise a particle, the particle was regarded to be composed of just that chemical species. Third, for particles internally mixed with two or more chemical species, particles were grouped according to the largest content. For example, an aluminosilicate particle with substantial amount of $CaCO_3$ was denoted $AlSi/CaCO_3$.

Since the presence of hydrogen cannot be detected in EPMA, organic components in atmospheric aerosols cannot be specified. Therefore, the speciation of carbonaceous particles was carried out in a somewhat arbitrary way; based on the C and O contents in individual particles, carbonaceous particles were classified into three groups, i.e., organic, carbon-rich, and

biogenic. When the sum of the atomic concentration of C and O was more than 90%, the particle was classified as organic. Among them, if the concentration of C was three times larger than that of O, the particles were classified as carbon-rich. Particles were classified as biogenic (such as pollen, spore, algae, and plant and insect fragments) when the atomic fractions of C and O were similar (within 10% deviation), and some N, P, S, K and/or Cl, the characteristic elements for biogenic particles, were included in the particle. Therefore, the carbon-rich particles are somewhat related to elemental carbon (EC) particles, whereas the biogenic particles can be regarded as one type of organic carbon (OC) particles. The analytical procedure for determining chemical species and the way to perform classification are described in more detail elsewhere (Ro *et al.*, 2000, 1999).

3. 4 Expert System for the Classification of Particles

The low-*Z* particle EPMA technique that provides the morphology, size, and chemical species of individual micro-particle is a useful technique for the characterization of environmental aerosols. However, in order to make a meaningful observation for real atmospheric aerosol samples, the analysis of a large number (at least several hundred) of particles is required to provide relevant statistics on the population of particles in the sample. To classify a large number of particles in a sample, a systematic methodology is necessary. When a computer program utilizes computational techniques that try to simulate human reasoning to solve complex problems, it is called an expert system. With the advent of fast, powerful, and inexpensive computers in the last decades, many applications of expert systems to solve specific problems have appeared in various research fields (Zhang and Chait, 2000; Koutny and Yeung, 1993; Harrington *et al.*, 1989).

An expert system that can reliably perform chemical speciation of particles analyzed by low-*Z* particle EPMA was developed (Ro *et al.*, 2004), that tries to mimic the logics used by experts and was implemented by applying macro programming available in MS Excel software. The expert system runs on IBM-PC compatible computers and uses input and output files in the format of MS Excel files. Its feasibility was verified for standard particles with known compositions and real atmospheric aerosols. By applying the expert system, the time necessary for the chemical speciation became shortened very much and data that contain detailed information could be saved and extracted later when more information was needed for further analysis. After running the expert system for a sample, the size-segregated number concentrations of various chemical species could be obtained.

4. CHARACTERIZATION OF ATMOSPHERIC AEROSOLS USING LOW-*Z* PARTICLE EPMA

The low-*Z* particle EPMA has been applied to characterize various types of aerosol particles for the last decade. Herein, several typical applications are introduced to demonstrate its feasibility of the low-*Z* particle EPMA for the detailed characterization of real ambient aerosol samples.

4. 1 Asian Dust

4. 1. 1 Introduction

Nearly every spring, usually from March to May, "Asian Dust" originated from the arid areas of Central China has been transported into Eastern China, Korea, Japan, and even to the Pacific Ocean. The elevated levels of particulate matter (PM) during dust storms affect the human health, the visibility, and industrial activities. While the dust particles travel long-distance, they can react with diverse chemical species and/or provide a reaction site for chemicals in the atmosphere. Therefore, Asian Dust can possibly carry other chemical species along with the original soil components. For example, it would react with the atmospheric pollutant gases such as SO_x and NO_x, thus the transport of the reacted dust particles to the East Asian region could result in the deposition of sulfates and nitrates, in addition to mineral dust. The modified Asian Dust particles can affect the global climate, since the direct radiative forcing properties of the dust particles can be changed. Also their effectiveness to serve as cloud condensation nuclei can be altered. Hence, increasing attention has been devoted to the study of physicochemical characteristic changes of Asian Dust particles during long-range transport. In this section, the variation of the physicochemical properties of Asian dust aerosol samples collected during four dust storm events in Korea is discussed.

4. 1. 2 Sampling and Measurements

Four sets of Asian Dust aerosol samples were collected in ChunCheon, Korea on March 7 and April 7 in 2000 and March 22 and May 17 in 2001 (These four samples were notated as "March_00", "April_00", "March_01", and "May_01" samples, respectively). ChunCheon with the population of 200,000 is a small city with a wide suburban area. Back-trajectories for the four Asian Dust events are shown in Fig. 1 (The back-trajectory analyses were performed by

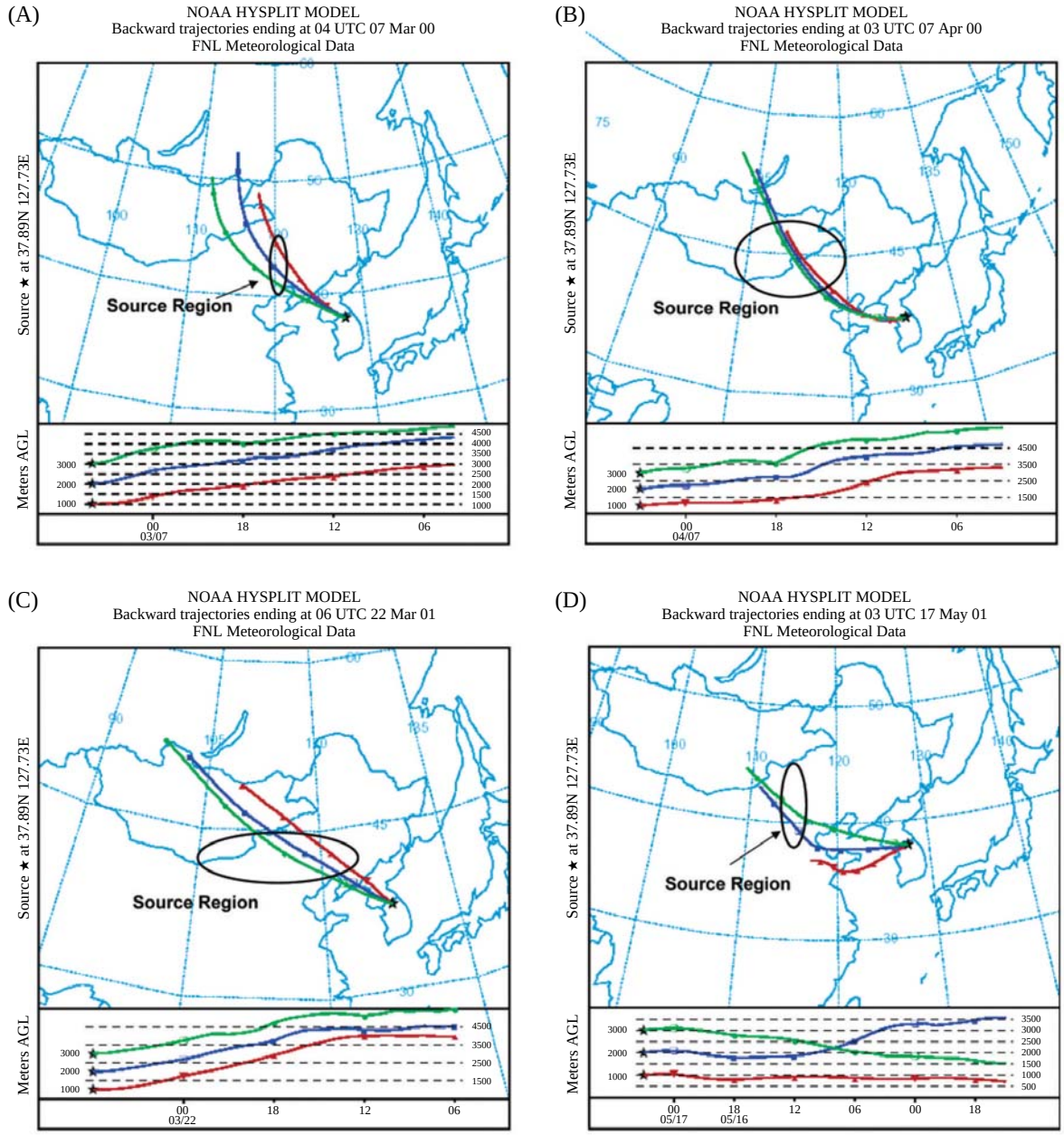

Fig. 1. Air-mass backward trajectories for Asian Dust samples collected on (A) March 7, 2000, (B) April 7, 2000, (C) March 22, 2001, and (D) May 17, 2001. Reprinted from permission from ref. Ro *et al.*, 2005. Copyright 2005 American Chemical Society.

using the HYSPLIT model and meteorological data available on the NOAA/ARL website). The circularly marked regions in the figure are the source regions of the Asian Dust storm. Samplings were done in the middle of the dust storms by using a seven-stage May cascade impactor. Some 300 particles for each stage sample were analyzed. The particles on the seventh stage were not analyzed because the sizes of particles were too small to be analyzed by SEM/EDX.

4.1.3 Results and Discussion

Figs. 2-5 show the size dependent relative abundances of chemical species observed in the Asian Dust samples (the aerodynamic cut-offs of stages 1-6 in May impactor are 16, 8, 4, 2, 1, and 0.5, respectively). The relative abundances of each chemical species in a stage sample were obtained by dividing the number of the chemical species by the number of the analyzed particles. The major chemical species found in the Asian Dust particle samples were aluminosilicate,

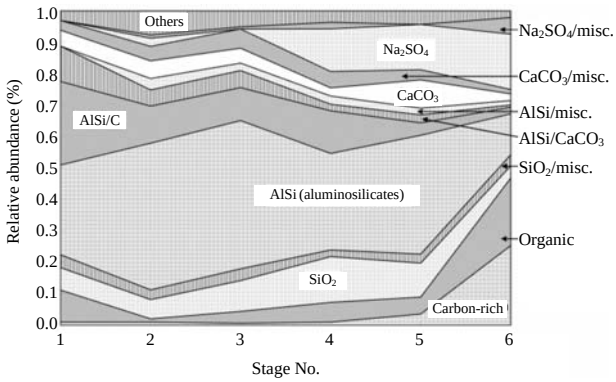

Fig. 2. Relative abundances of each chemical species in the "March_00" Asian Dust sample (Cut-off diameters of stages 1-6 are 16, 8, 4, 2, 1 and 0.5 μm, respectively). Reprinted from permission from ref. Ro *et al.*, 2005. Copyright 2005 American Chemical Society.

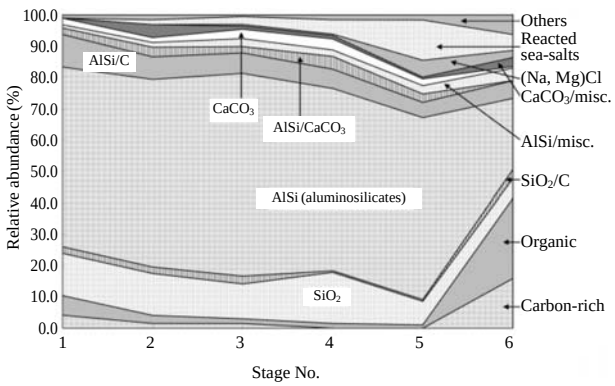

Fig. 3. Relative abundances of each chemical species in the "April_00" Asian Dust sample (Cut-off diameters of stages 1-6 are 16, 8, 4, 2, 1 and 0.5 μm, respectively). Reprinted from permission from ref. Ro *et al.*, 2005. Copyright 2005 American Chemical Society.

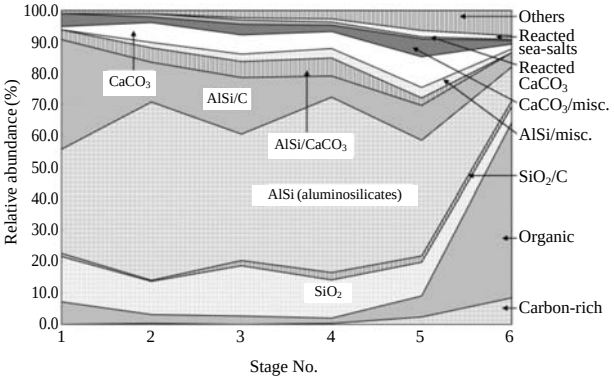

Fig. 4. Relative abundances of each chemical species in the "March_01" Asian Dust sample (Cut-off diameters of stages 1-6 are 16, 8, 4, 2, 1 and 0.5 μm, respectively). Reprinted from permission from ref. Ro *et al.*, 2005. Copyright 2005 American Chemical Society.

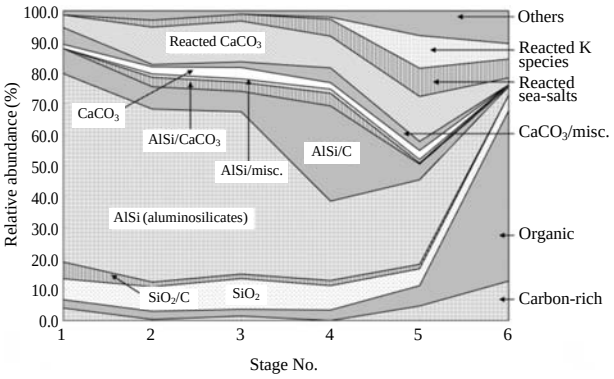

Fig. 5. Relative abundances of each chemical species in the "May_01" Asian Dust sample (Cut-off diameters of stages 1-6 are 16, 8, 4, 2, 1 and 0.5 μm, respectively). Reprinted from permission from ref. Ro *et al.*, 2005. Copyright 2005 American Chemical Society.

silicon dioxide, calcium-containing, marine-originated, and carbonaceous (specified either as organic or carbon-rich) particles. Overall, the soil-derived particles such as aluminosilicate, silicon dioxide, and calcium-containing particles were the most common in the Asian Dust samples.

Aluminosilicates and Silicon Dioxide

There exists so many different types of aluminosilicate particles as they contain a small amount (less than 5% in atomic concentration) of Na, Mg, S, Cl, K, Ca, and Fe. All these particles were simply grouped as "AlSi (aluminosilicates)". The particles classified as "AlSi" could be one of typical aluminosilicate minerals such as feldspar or clay mineral. It was observed that many aluminosilicate particles contain carbonaceous species which probably comes from humic substances in soil (Ro *et al.*, 2000). In this case, they were grouped as "AlSi/C". Some aluminosilicate particles existed as a mixture with $CaCO_3$, $MgCO_3$, Fe_2O_3, $CaSO_4$, Na_2SO_4, or $MgSO_4$. Since particles internally mixed with aluminosilicates and $CaCO_3$ were significant in number, they were marked as "AlSi/$CaCO_3$". Other mixtures were grouped as "AlSi/misc.". In all samples, aluminosilicate-containing particles were the most abundant in all size ranges except stage 6. For the stage 6 samples (D_p: 0.5-1 μm), carbonaceous particles were the most abundant. In Fig. 6, overall relative abundances of the significantly encountered particle types in the four samples are shown. The overall relative abundance was calculated by dividing the number of the specific type of particles by the

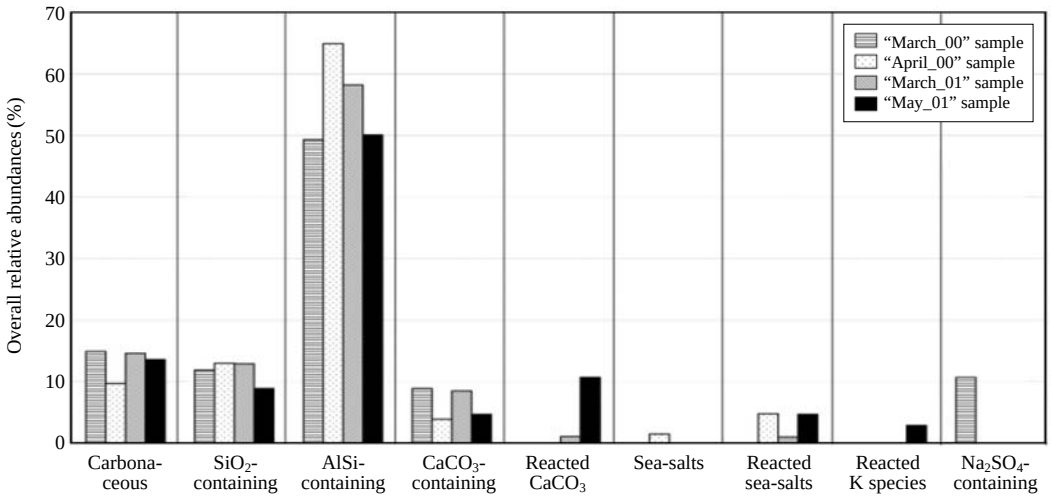

Fig. 6. Overall relative abundances of the major particle types in Asian Dust samples. Reprinted from permission from ref. Ro *et al.*, 2005. Copyright 2005 American Chemical Society.

total number of analyzed particles for each sample. As shown in Fig. 6, the relative abundances of aluminosilicate-conatining particle in all samples are overwhelmingly large: the "April_00" sample and "March_01" sample contain more than 60% of aluminosilicate particles. These two samples also contain SiO_2-containing particles more than other two samples. In addition, most of the aluminosilicate-containing particles in the "April_00" sample were found as a single species of aluminosilicate without mixing with other chemical species. The compositional difference in aluminosilicate particles might reflect the characteristics of the soils of the source regions. SiO_2-containing particles were the second most abundantly encountered soil-derived ones (see Fig. 6) and their relative abundances were in the range of 5-18% depending on the size and the samples.

Calcium-containing Particles

$CaCO_3$-containing particles were encountered with the relative abundances of 2-20%, depending on the size and the sample. Since $CaCO_3$ can react with SO_x and NO_x to produce $CaSO_4$ and $Ca(NO_3)_2$, respectively, it is of great interest to investigate the potential chemical modification of the Asian Dust during its long-range transport. The $CaCO_3$-containing particles were grouped into four types, i.e., "$CaCO_3$", "AlSi/$CaCO_3$", "$CaCO_3$/misc.", and "reacted $CaCO_3$". "AlSi/$CaCO_3$" particle is a mixture of aluminosilicates and $CaCO_3$. When a particle was found as an internal mixture of $CaCO_3$ and other chemical species such as $MgCO_3$, SiO_2, Fe_3O_3, or carbonaceous species, it was classified as a "$CaCO_3$/misc." particle. The products of atmospheric reaction between $CaCO_3$ and SO_x/NO_x, mostly $CaSO_4$ or $Ca(NO_3)_2$ or their mixtures, were classified as "reacted $CaCO_3$" particles.

As shown in Figs. 4 and 5, the overall relative abundances of particles of "$CaCO_3$-containing" and "reacted $CaCO_3$" groups are 9.5% and 0.9%, respectively, for the "March_01" sample and 4.7% and 10.7%, respectively, for the "May_01" sample. Here, the "$CaCO_3$-containing" group is for particles that contain $CaCO_3$ species without sulfate and/or nitrate. The "May_01" sample seemed to have experienced very dramatic chemical modification of $CaCO_3$ species because the number of particles for the "reacted $CaCO_3$" group was much larger than that of the un-reacted $CaCO_3$ particles. In addition, the reacted $CaCO_3$ particles were observed significantly even in stages 1-3 where coarse particles were collected. This means that the sample in question had enough reaction time and reactants to consume even for relatively large $CaCO_3$ particle. Among 13 reacted $CaCO_3$ particles found in the "March_01" sample, the numbers of particles that contain $Ca(NO_3)_2$ and $CaSO_4$ were 6 and 7, respectively. For this sample, $CaCO_3$ reacted with NO_x and SO_x in a similar extent. However, for the "May_01" sample, among 142 reacted $CaCO_3$ particles, particles containing $Ca(NO_3)_2$ outnumbered those containing $CaSO_4$ (128 vs. 36).

The reacted $CaCO_3$ particles were hardly found for the "March_00" and "April_00" samples, therefore it was assumed that these samples had not experienced atmospheric reactions during their long-range transport. By analyzing the chemical composition of the $CaCO_3$-containg particles, we can see the difference in the extent of chemical modification between samples. "May_01" sample did show the extensive chemi-

cal modification of $CaCO_3$ species and the "March_01" showed a significant chemical modification. On the other hand, the "March_00" and "April_00" did not at all. The reason for these differences for the samples is not clear, but it is certain that many factors such as meteorological conditions and the concentrations of gaseous sulfur and nitrogen species in areas that the air-masses passed through play important roles in chemical modification during long-range transport.

Marine Particles

It was well demonstrated that "genuine" and "reacted" sea-salts can be clearly distinguished by the low-*Z* particle EPMA (Ro *et al.*, 2001b). Since the sea water contains Mg, the Mg X-ray peak was detected when the genuine sea-salt particles were investigated. Therefore, the genuine sea-salt particles were classified as (Na, Mg)Cl. The reacted sea-salts were mostly sodium nitrate and/or sulfate. The particles of sea origin can be verified by the existence of residual Cl in the X-ray spectrum. For the "March_00" sample, either genuine or reacted sea-salts were not significantly observed. It might be due to the fact that the air-mass for the sample did not pass over the Yellow Sea (see Fig. 1(A)). However, for other samples that had passed over the Yellow Sea, a significant number of sea-salt particles were observed. The overall relative abundances of marine-originated particles for the "April_00", "March_01", and "May_01" samples were 6.3%, 0.9%, and 4.7 %, respectively. For the "April_00" sample, the reacted sea-salts outnumbered the genuine sea-salts (4.8% vs. 1.5%). Regarding the $CaCO_3$-containing particles, it is interesting to notice that the reacted $CaCO_3$ particles were not significantly observed for this sample. The "March_01" sample entrained the least amount of sea-salts particles among the three samples, and only the reacted sea-salts were observed. Again, the reacted $CaCO_3$ particles were outnumbered by the un-reacted $CaCO_3$ particles for this sample. This implies that sea-salts had experienced their chemical modification more rapidly and extensively than $CaCO_3$ particles. Most of the reacted sea-salt particles were encountered in stages 4-6 (where the fine particles were collected), and it might be due to the larger surface-to-volume ratio for the smaller particles. The "May_01" sample also contains only the reacted sea-salts. Since most of reacted sea-salt and reacted $CaCO_3$ particle were observed as the products of atmospheric reaction, particles in this sample seemed to experience the most extensive chemical modification among the four Asian dust samples.

Among 50 reacted sea-salt particles in the "April_00" sample, the numbers of particles that contain nitrate and sulfate are 13 and 38, respectively. For the "March_01" sample, among 14 reacted sea-salt particles, the numbers of particles that contain nitrate and sulfate are 5 and 11, respectively. For these samples, sea-salt particles reacted with SO_x to a greater extent than with NO_x. However, for the "May_01" sample, among 64 reacted sea-salt particles, particles containing nitrate outnumber those containing sulfate (55 vs. 18). This tendency is similar to that for the reacted $CaCO_3$ particles observed in the "March_01" and "May_01" samples, where nitrate- and sulfate-containing reacted $CaCO_3$ particles were observed in a similar extent for the "March_01" sample, and yet nitrate-containing particles outnumber sulfate-containing particles for the "May_01" sample. The "May_01" sample must have experienced a situation in which nitrate was produced more easily than sulfate.

Potassium-containing Particles

The "May_01" sample has another unique feature in terms of the presence of reacted potassium-containing particles. The reacted potassium-containing particles included sulfate, nitrate, carbonate, and mixtures of sulfate, nitrate, and/or carbonate such as K_2SO_4, KNO_3, $K(NO_3, SO_4)$, $K(CO_3, SO_4)$, $K(CO_3, NO_3)$, $K(CO_3, NO_3, SO_4)$. Among 37 potassium-containing particles, chemical species of 15 particles was K_2SO_4, that was the most abundant among the potassium-containing particle types. These K_2SO_4 particles are not natural mineral particles because 12 particles among 15 particles classified as K_2SO_4 appeared to contain a small amount of nitrate in them when their X-ray spectral data were examined in detail. Even though no single K_2CO_3 particle was encountered, it is certain that K_2CO_3 particles reacted in the atmosphere to produce reacted potassium-containing particles. The reason is that the K_2CO_3 species was often found as mixtures of K_2SO_4 and/or KNO_3, implying that atmospheric reaction for those particles was not completed. The reacted potassium-containing particles were mostly encountered in stages 5 and 6 (D_p: 0.5-2 μm). Among the 37 potassium-containing particles, sulfate-containing particles outnumbered nitrate-containing ones (34 vs. 13). As stated before, for the reacted $CaCO_3$ and sea-salt particles in this sample, nitrate-containing particles outnumber sulfate-containing ones, which is opposite to that for reacted potassium-containing particles. It is not possible to explain the discrepancy between these observations, but it is certainly related to the reactivity of each chemical species. There has not been any report regarding chemical modification of K_2CO_3 during long-range transport of Asian Dust. In this work, it is clearly shown that K_2CO_3 species, in addition to $CaCO_3$ species and sea-salts, is also important in the study of chemical modification of Asian Dust during transport.

Carbonaceous Particles

In all samples, carbonaceous particles such as organic and carbon-rich were significantly encountered in the stages 5 and 6 (D_p: 0.5-2 μm). It is well known that anthropogenic carbonaceous and ammonium sulfate particles are major chemical species in urban atmospheric aerosols (Ro *et al.*, 2002), thus it can be assumed that the carbonaceous particles might be from local anthropogenic sources. However, in these samples, ammonium sulfate particles were rarely observed, which implies that these carbonaceous particles could be a part of the Asian Dust particles entrained during their transport.

4.2 Urban Aerosols

4.2.1 Introduction

For typical urban aerosols, a significant portion of aerosols is anthropogenic in origin. The gaseous SO_x and NO_x emitted from industry and mobile combustion engines cause the production of secondary aerosols such as sulfate and nitrate. Chemical composition of urban aerosols can be variable depending on the surrounding environment, such as population and the geography. Compositions of atmospheric aerosols in three cities in Korea, namely Seoul, CheongJu, and ChunCheon, were investigated. Seoul, the capital of Korea, is a megacity with high population (population: 10.3 million, area: 605 km^2), whereas CheongJu is relatively small (population: 0.57 million, area: 153 km^2) and has industrial complexes in the city. ChunCheon is the least densely populated (population: 0.25 million, area: 1,116 km^2) among the three, and is free of industrial complexes. The three cities have different urban characteristics in terms of their population, size, and industrial circumstances. The results of single particle analysis for the three cities having different environment were expected to provide the detailed information on their atmospheric characteristics.

4.2.2 Sampling and Measurement

All the samplings were done during the winter of 1999. In Seoul, the sampling was done on December 11, 1999, on the roof of St. Mary's Hospital building (30 m above ground level), which is located at the Youido district in central Seoul. In ChungJu, the sample was collected on the roof of a campus building of ChungBuk National University (3 m above ground level) on November 13, 1999. The campus is located in downtown CheongJu. Industrial complexes inside the city of CheongJu are just 2 km north from the sampling site. In ChunCheon, the sampling was performed on the roof of a campus building of Hallym University (12 m above ground level) on November 27, 1999.

Particles were sampled on Ag foil (99.95%, 0.025 mm, Goodfellow) using a seven-stage May cascade impactor. For each sample, some 300 particles for each stage in #1-6 were analyzed. The particles on the seventh stage were not analyzed because the sizes of particles were too small to be analyzed by SEM/EDX. Since the samples were stored for a couple of months before the analysis, it might be possible that some of semi-volatile particles such as ammonium nitrate could have partially been lost during storage. The measurements were carried out on a JEOL 733 electron probe micro-analyzer equipped with an Oxford Link SATW ultra-thin window EDX detector.

4.2.3 Results and Discussion

The relative abundances of the chemical species found in atmospheric aerosols collected in Seoul, ChungJu, ChunCheon are shown in Figs. 7-9. The major chemical species encountered in urban atmosphere were: carbonaceous particles (specified either as organic, carbon-rich, or biogenic), aluminosilicate, silicon dioxide, calcium carbonate, iron oxide, marine-originated (such as sodium chloride and sodium nitrate), and ammonium sulfate particles. It is well known that these types of particles are common in urban atmospheres (Polissar *et al.*, 2001; Zhang and Friedlander 2000; Hughes *et al.*, 1999; Chow *et al.*, 1992; Van Borm and Adams, 1989). The size dependences of the population of the chemical species are clearly shown in Figs. 7-9. In general, soil derived particles, e.g. aluminosilicates, silicon dioxide, calcium carbonate, and iron oxide, and also sea salts were mainly observed in the coarse fraction (i.e., on impactor stages 1-3, where their cut-offs are 16, 8, and 4 μm, respectively), while carbonaceous and ammonium sulfate particles that may have anthropogenic origin were the major species in the fine fraction (in stages 4-6, where their cut-offs are 2, 1, and 0.5 μm, respectively).

Carbonaceous Particles

They were found both in coarse (stages 1-3) and fine fractions (stages 4-6). In terms of the particle size, most of carbonaceous particles in coarse fraction might be naturally emitted and those in fine fraction might be anthropogenic. Observation of the organic particles mostly in the fine fraction implies their anthropogenic origin. Biogenic organic particles such as pollen were found as coarse particles in stages 1-3. In the Seoul and ChunCheon samples, the carbonaceous particles were ca. 60% in stage 6, i.e., the majority of the finest particles were carbonaceous particles. Whereas, in the CheongJu sample, ammonium sulfate was the main component in the fine fraction (ca. 70%

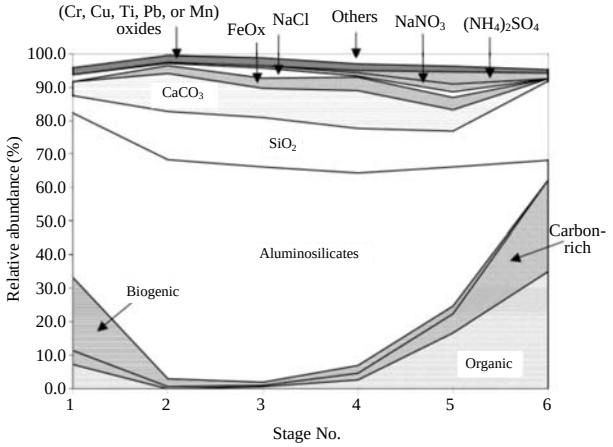

Fig. 7. Relative abundances of each chemical species in the Seoul sample (Cutoff diameters of stages 1-6 are 16, 8, 4, 2, 1, and 0.5 μm). Reprinted from permission from ref. Ro *et al.*, 2002. Copyright 2002 American Chemical Society.

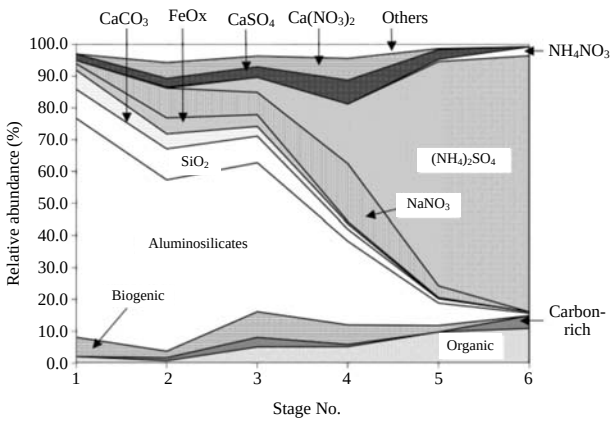

Fig. 8. Relative abundances of each chemical species in the ChungJu sample (Cutoff diameters of stages 1-6 are 16, 8, 4, 2, 1, and 0.5 μm). Reprinted from permission from ref. Ro *et al.*, 2002. Copyright 2002 American Chemical Society.

in stage 5 and ca. 80% in stage 6), and the relative abundance of the carbonaceous particles was overwhelmed by sulfate particles. Detailed discussion on the sulfate particles will be given below.

Aluminosilicate and Silicon Dioxide Particles

They have been observed abundantly in urban atmosphere and mostly regarded as soil-derived, being resuspended by mechanical forces such as running automobiles, strong winds, and construction activities. The aluminosilicate particles were abundantly encountered in coarse fraction (in stages 1-3) of all samples (see Figs. 7-9). However, in the Seoul sample, they were significantly found even in stages 5 and 6.

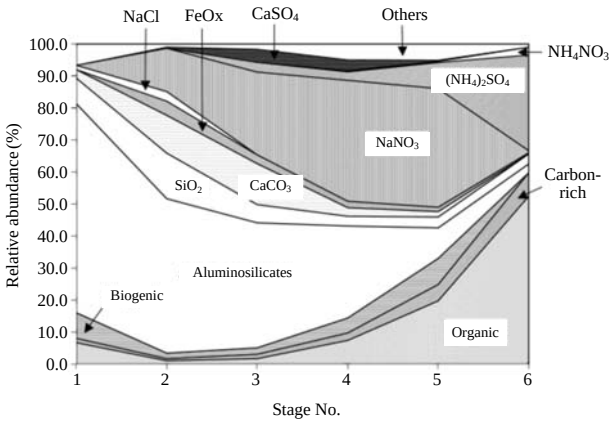

Fig. 9. Relative abundances of each chemical species in the ChunCheon sample (Cutoff diameters of stages 1-6 are 16, 8, 4, 2, 1, and 0.5 μm). Reprinted from permission from ref. Ro *et al.*, 2002. Copyright 2002 American Chemical Society.

Similarly, silicon dioxide particles were significantly present in all stages for the Seoul sample, whereas they were mostly encountered in stages 1-3 for the CheongJu and ChunCheon samples. Zhang and Friedlander (2000) reported that $PM_{2.5}$ and $PM_{2.0}$ urban particles collected in various cities of China also had high silica contents (ca. 18%) next to carbonaceous and ammonium sulfate and the concentrations of the fine silica component in Beijing and Lanzhou, China, were 26-36 times higher than those in Los Angeles, USA. They claimed that the fine silica probably came from coal combustion, crustal sources, and rice straw burning. Silicon dioxide and aluminosilicate particles in the Seoul sample seemed to have two sources, namely soil-derived and anthropogenic. In other study (Ro *et al.*, 2001a), soil-derived silicon dioxide particles in the coarse fraction usually were observed to contain small amount of aluminum (possibly from aluminosilicate) and/or carbon (from humic substance in soil) elements. However, silicon dioxide particles in stage 6 in Seoul sample might be fly ashes since they were "pure". A possible local source of anthropogenic silicon oxide particles is an incinerator (location: Mok-dong, Seoul; daily capacity of 550 ton; average running rate of 60%) located 3 km west from the sampling site.

Calcium-containing Particles

They were observed as carbonate, sulfate, and nitrate. As shown in Figs. 7-9, calcium carbonate particles were significantly encountered in the coarse fraction of all the samples. However, there were some differences in their size distributions among the samples. In the Seoul sample, the relative abundance of the $CaCO_3$ particles was relatively constant in all stages.

In the ChunCheon sample, $CaCO_3$ particles were significantly observed in stages 1-3 and not in the fine fraction (stages 4-6). This finding implies that most of the calcium carbonate particles in the ChunCheon sample were soil-derived. In the CheongJu sample, the overall relative abundance of the Ca-containing particles was smaller than that of others and, in addition, fine calcium carbonate particles were not encountered. The two types of calcium-containing particles, namely sulfate and nitrate, were significantly observed only in the CheongJu sample. Calcium nitrate particles were significantly encountered in stages 2-4, whereas, sulfate in stages 1-5. The formation of $Ca(NO_3)_2$ by the reaction between $CaCO_3$ and HNO_3 was proposed (Dentener *et al.*, 1996) and directly observed (Carmichael *et al.*, 1997). A recent study claimed that soil-derived aerosol particles were more suitable for the internal mixture of sulfate and nitrate than the other kinds of particles, and this claim was based on analyzing individual particles with the combination of microchemical test and EPMA techniques (Zhang *et al.*, 2000). Other study reported the observation of the internal mixtures of $CaCO_3$ and $Ca(NO_3)_2$ (Ro *et al.*, 2001a). It seemed that the reaction had not completely occurred for these particles. In addition, since some of the $Ca(NO_3)_2$ particles also contained small amount of aluminosilicates, $Ca(NO_3)_2$ seemed to be most probably the product of a reaction between anthropogenic nitric acid and soil-derived $CaCO_3$ species. In the ChungJu sample, about 30% of Ca-containing particles were found as internal mixture of $CaCO_3$ and $Ca(NO_3)_2$ species. In addition, observation of some calcium sulfate particles including calcium nitrate and/or carbonate species implies that some of the calcium sulfate particles were also formed by an atmospheric reaction.

Iron Oxide Particles

They constituted ca. 2.0% of total analyzed particles. Iron oxides could be originated from soil or anthropogenic emissions (e.g. as fly-ash). Iron oxides were observed in stages 2-5; for the Seoul sample, the particles were more abundantly encountered in stages 4 and 5 (more in the fine fraction), whereas in the CheongJu and ChunCheon samples, the particles were more abundantly observed in stages 2 and 3 (more in the coarse fraction). It implies that the iron oxide particles in the Seoul sample might be originated from anthropogenic emission. The observation of anthropogenic fine SiO_2 particles in the Seoul sample supports the assertion. Studies carried out on urban particles in Europe reported quite abundant iron oxide particles in the air (Van Borm *et al.*, 1990). In the study on aerosols in Antwerp, Belgium, using the low-*Z* EPMA, the iron oxide particles were believed to have two sources, namely soil and anthropogenic, although the anthropogenic source was not determined (Ro *et al.*, 2000).

Marine Particles

They were observed as "genuine" or "reacted" ones. Since sea-water contains significant amount of Mg (the mole ratio of Mg to Na in sea-water is 0.12 to 1 (Weast *et al.*, 1984)), the Mg peak can be seen in their X-ray spectrum when marine-originated particles are analyzed using EPMA. All the NaCl particles in the sample were found to be genuine sea-salts and most of $NaNO_3$ particles also contain Mg in them. Furthermore, the observation of the existence of residual Cl in $NaNO_3$ particles might be the direct evidence of the heterogeneous atmospheric reaction between the sea-salt particle and gaseous NO_x in the air. Gard *et al.*, (1998) reported that the atmospheric reaction between sea-salts and HNO_3 to produce $NaNO_3$ occurred in a relatively short time (on a time scale of about a half day). Observation of overwhelmingly abundant $NaNO_3$ particles over genuine sea-salts in the CheongJu and ChunCheon samples implies that the air-masses had spent a sufficient time in the air. However, lack of Na_2SO_4 particles implies that sulfate formation from the sea-salts does not occur as easily as that of nitrate. The similar observation that the Na_2SO_4-containing particles were much less abundant than the NaCl- and $NaNO_3$-containing particles was seen for the aerosol samples collected in Cheju Island, Korea (Ro *et al.*, 2001b).

Ammonium Sulfate Particles

They were observed in the fine fraction (stages 4-6) for all the three samples (see Figs. 7-9). It is well known that ammonium sulfate particles in the air are anthropogenic and they are the major fine particles which can be found in urban atmosphere. The ammonium sulfate particles were most abundantly encountered in the CheongJu sample, and significantly in the ChunCheon sample, but relatively less in the Seoul sample. In addition, in the CheongJu sample, some ammonium sulfate particles were found even in the coarse fraction (i.e., on stage 3). As discussed previously on the Ca-containing particles in the ChungJu sample, most of Ca-containing particles were observed as nitrate and/or sulfate without carbonate particles. It seemed that there was an anthropogenic emission during the sampling period in ChungJu (ChungJu has an industrial complex in the city.).

4.3 Subway Aerosol

4.3.1 Introduction

Many people within the worldwide metropolitan

areas commute using underground subway transportation and spend considerable time in the underground subway environment on a daily basis. The atmospheric environments of underground subway stations have relatively unique characteristics since there is a peculiar source of aerosol by the movement of train and the ventilation is restricted. Therefore, there has been increasing attention to air quality in the underground subway system because of its possible adverse influence on public health (Karlsson *et al.*, 2006; Karlsson *et al.*, 2005; Seaton *et al.*, 2005; Chillrud *et al.*, 2004). Due to the limited ventilation, in general, the PM concentrations of the underground subway system are higher than those of outdoor atmosphere. It has been reported that the PM_{10} concentrations in various subway stations around the world were a few times higher than those of ambient outdoor atmosphere (Branis, 2006; Aarnio *et al.*, 2005; Johansson and Johansson, 2003; Furuya *et al.*, 2001). Since PM emission sources in the underground subway stations are very different from those in outdoor urban environments, the chemical compositions of subway particles are unique. Subway particles are dominated by Fe and Si, and contain Mn, Cr, Cu, Ca, and K as minor components (Salma *et al.*, 2007; Birenzvige *et al.*, 2003; Sitzmann *et al.*, 1999). In particular, concentrations of Fe, Mn, and Cr in $PM_{2.5}$ samples collected in underground subway stations of New York City were found to be more than 100 times higher than those in aboveground ambient samples (Chillrud *et al.*, 2004). Studies have shown that the subway particles were more genotoxic and more likely to induce oxidative stress in cultured human lung cells than the particles from welding fume and the wood combustion (Karlsson *et al.*, 2006; Karlsson *et al.*, 2005; Seaton *et al.*, 2005).

Herein, subway particles collected in Hyehwa station, one of the underground subway stations in Seoul, Korea were investigated. The Seoul subway system contained 8 lines with a total of 327 stations in 2005. According to statistics provided from the Seoul metro transportation center (http://www.seoulmetro.co.kr), approximately 6.7 million commuters use the Seoul subway system on a daily basis. The Hyehwa station is one of the busiest subway stations with 58,000 commuters per day. In 2005, the average PM_{10} in Seoul was 58.0 $\mu g/m^3$ and that in Hyehwa station was 121.5 $\mu g/m^3$. By the combined use of the morphological and chemical information obtained from the low-*Z* particle EPMA, it was observed that subway particles were mostly iron-containing particles which were originated from the wear processes at rail-wheel-brake interfaces (Kang *et al.*, 2008).

4.3.2 Sampling and Measurement

Sampling was done at the platform of the Hyehwa station using a 7-stage May cascade impactor. Subway particle samples were collected twice every season during 2004-2005: Dec. 16 and 17, 2004; May 3 and 5, July 4 and 6, and Nov. 23 and 25, 2005. The measurements were carried out using a Hitachi S-3500N environmental scanning electron microscope equipped with an Oxford Link SATW ultrathin window EDX detector. Due to the SEM resolution, particles on stage 1-5 were analyzed. About 300 particles for each stage were analyzed (1,300 particles for each sample).

4.3.3 Results and Discussion

Based on their chemical compositions, 4 major particle types were significantly encountered: Fe-containing; soil-derived; carbonaceous; and secondary nitrate and/or sulfate particles. In Table 1, overall relative abundances of those particle types for the 8 samples are shown. Since the particles collected on stages 1-5 were analyzed, the results shown in Table 1 is for the aerosols with $D_p > 1\,\mu m$. Fe-containing particles were overwhelmingly abundant (more than 60%) in the subway station environment. Other studies for the subway aerosols in London, New York, Helsinki, Tokyo, and Budapest have also reported the very high concentrations (above 42%) of iron (Salma *et al.*, 2007; Aarnio *et al.*, 2005; Chillrud *et al.*, 2004; Furuya *et al.*, 2001; Sitzmann *et al.*, 1999).

Fe-containing Subway Particles

They are shown as a secondary electron image in Fig. 10. In this study, Fe-containing particles were classified into three different types: iron metal (denoted as “Fe”), partially oxidized (denoted as “Fe/FeOx”), and fully oxidized (denoted as “FeOx”). A major advantage of EPMA technique is that the morphology of the particle can be obtained with the chemical composition. The combined information makes it possible to deduce the source of the particle. Most of Fe-containing particles were observed as oxidized form and some nano-sized iron oxide particles formed an agglomerated lump on the surface of Fe-containing particles (see particles (a)-(c) in Fig. 11B). Similar way to the formation of arc welding particles (Zimmer and Biswas, 2001), the nano-sized iron particles were probably formed by the condensation of gaseous iron species generated from the sparking between the third rail and the electricity guide of subway trains. Iron metal particles also can be produced by the mechanical friction process at the rail-wheel-brake interface. It is probable that the surface of the primary iron particles must be active enough so that oxygen in the air can easily react on the metallic surface, resulting in the formation of iron oxides. Since the surface area is

Table 1. Overall relative abundances of subway particle types observed in the 8 samples collected at the platform in Hyehwa station. Reprinted from permission from ref. Kang *et al.*, 2008. Copyright 2008 American Chemical Society.

Particle types	Dec. 16, 2004	Dec. 17, 2004	May 3, 2005	May 5, 2005	July 4, 2005	July 6, 2005	Nov. 23, 2005	Nov. 25, 2005
Iron-containing	60.5	71.5	70.8	71.4	79.1	78.0	71.1	74.6
Carbonaceous	13.2	7.7	9.0	9.2	10.5	8.6	5.4	7.4
Soil-derived (sum)	14.0	11.4	10.7	11.5	6.0	7.5	13.1	9.4
Aluminosilicates	5.1	4.6	3.8	3.8	2.0	2.6	4.6	2.5
Aluminosilicates/C	2.8	1.5	2.2	1.8	1.0	1.3	2.0	1.1
$CaCO_3$	0.8	1.0	0.1	0.7	0.5	0.7	1.5	1.0
$CaCO_3$/C	1.2	0.8	0.4	0.6	0.5	0.4	1.3	0.8
SiO_2	1.8	1.3	2.7	2.8	0.8	1.4	1.5	2.5
SiO_2/C	2.5	2.2	1.5	1.8	1.2	1.1	2.2	1.5
Secondary nitrates/sulfates (sum)	8.0	6.8	5.1	4.0	1.3	2.7	6.0	4.1
$Ca(NO_3, SO_4)$	4.2	2.5	1.5	2.2	0.8	1.1	2.6	1.2
$(Na, Mg)(NO_3, SO_4)$	1.5	1.0	3.6	1.8	0.5	1.2	3.2	2.7
$(NH_4)_2SO_4$	2.3	3.3	–	–	–	0.4	0.2	0.2
Others	4.2	2.6	4.5	3.9	3.1	3.3	4.3	4.5
Total	100	100	100	100	100	100	100	100

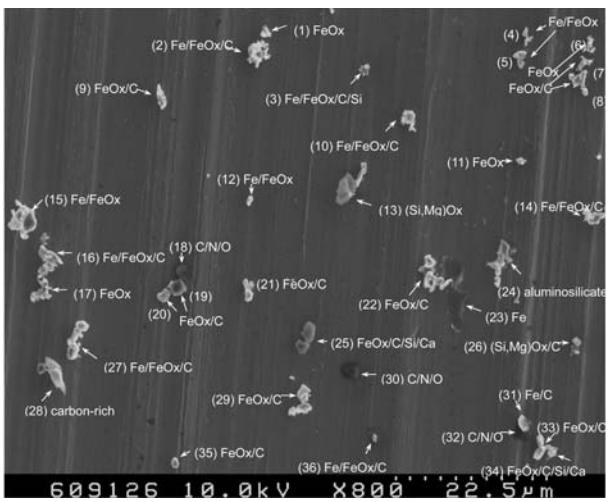

Fig. 10. A typical secondary electron image for subway particles collected at Hyehwa subway station in Seoul, Korea. Reprinted from permission from ref. Kang *et al.*, 2008. Copyright 2008 American Chemical Society.

larger for smaller particles, oxidized iron particles were more frequently encountered in fine fraction (on stages 4 and 5). In addition, the existence of gaseous iron species in the subway environment can be explained by the observation of minor iron species contained in almost all the subway particles, even for soil particles that came from outdoor.

Iron metal particles were clearly distinguishable from oxidized iron particles in the secondary electron images. Iron metal particles were observed mostly in the sliced form, implying that they were scraps peeled off from train wheels or rails (see Fig. 11A). In the secondary electron image, the iron metal particles look darker compared to iron oxides particles. The difference in brightness mainly results from the difference in the secondary electron yields between conducting metal and insulating oxide particles. The insulating oxide particles can develop a negative voltage by the accumulation of primary electrons, resulting in a bright contrast due to a larger emission of secondary electrons by repulsion (Goldstein *et al.*, 2003).

Many Fe-containing particles classified either as iron metal, partially, or fully oxidized iron oxides usually contained small amount of C, N, Mg, Al, Si, S, and/or Ca. When the atomic concentrations of those elements were larger than 10%, the elements were regarded as major chemical species. For example, the notation of "FeOx/C/Si/Ca" for particles #25 and #34 in Fig. 10 indicates that the particles are iron oxides internally mixed with C, Si, and Ca species. Using single particle analysis, Sitzmann *et al.* (1999) discussed in depth the sources of subway particles containing C, Si, and/or Ca together with Fe: (a) particles containing both Fe and Si were generated from the friction between brake block composed of iron and glass fibers and train wheels, (b) particles containing Fe and Ca together were also generated in the same way because brake blocks contain $CaCO_3$, and (c) C element was from cast iron used for wheels and rails. In this study, these elements were also very frequently encountered in Fe-containing subway particles. For example, among 29 Fe-containing particles in Fig. 10, 22 particles contained Si and 12 particles contained Ca. According to Korean Standard Database (http://www.standard.go.

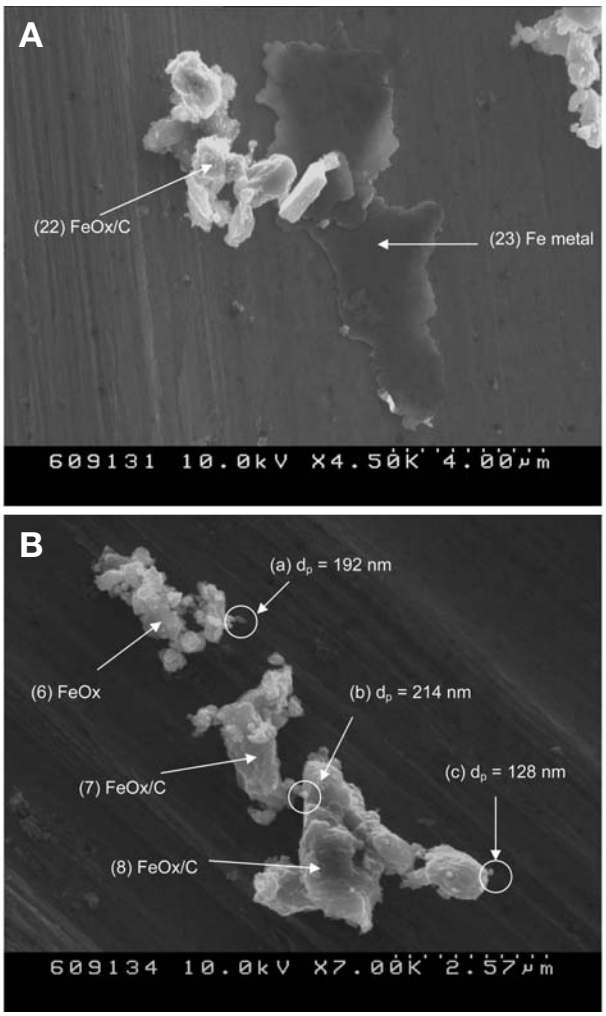

Fig. 11. Magnified Fe-containing particles shown in Fig. 10. Reprinted from permission from ref. Kang *et al.*, 2008. Copyright 2008 American Chemical Society.

kr), cast irons used for rails and wheels contain C (0.5-0.7%), Si (0.1-0.35%), Mn (0.6-0.95%), P (< 0.045%), and S (< 0.05%). Since the contents of carbonaceous species in Fe-containing subway particles are much higher than those of cast iron, the extra carbon observed in subway particles must come from the heterogeneous oxidation reaction of volatile organic carbons (VOCs) in indoor subway environment on the active surface of Fe-containing particles when the particles are generated during the wear process. The reaction of VOCs with Fe-containing particles explains why C element is observed in almost all Fe-containing particles.

Among the four seasonal samples, the summertime samples showed the most abundant Fe-containing particles. Other studies have reported similar observation that the concentrations of Fe-containing particles were higher in the summer than in the winter (Adams *et al.*, 2001a, b). Since whole areas of the Hyehwa subway station were air-conditioned during summertime, it is likely due to less air-exchange between indoor and outdoor areas. In general, it showed that the morning samples contained more abundant iron-containing particles than the afternoon samples. Three samples (Dec. 17, July 4, and Nov. 25) were collected in the morning and others in the afternoon. A reason for the observation of more abundant Fe-containing particles in the morning samples can be that the accumulated Fe-containing particles overnight drift in the air due to the movement of train. In addition, the frequency of train runs in the morning was greater (12 times/hour) than that in the afternoon (10 times/hour). Similar observations were reported in other studies; the PM in subway was proportional to the train passing frequency and reached a maximum during rush hour (Birenzvige *et al.*, 2003).

Carbonaceous Particles

They were significantly encountered with their relative abundances ranging in 5.4-13.2% (see Table 1). Since hydrogen cannot be detected in the low-*Z* particle EPMA, it has a limitation on the speciation of organic particles. Thus, particles were simply classified as carbonaceous particles when the sum of the atomic % of the carbon, nitrogen, and oxygen in the particle was larger than 90%. It was suggested that carbonaceous species in subway particles could originate from the carbon contained in cast iron (Sitzmann *et al.*, 1999). In that case, it is expected that carbonaceous species should be combined with Fe-containing particles. Indeed, many Fe-containing particles also contained carbon and those were classified as Fe-containing particles. However, the particles classified as carbonaceous particles were mostly composed of carbon, nitrogen, and oxygen without iron. It is likely that these anthropogenic carbonaceous particles came from the urban outdoor atmosphere.

Soil-originated Particles

Soil-originated particles such as aluminosilicates, SiO_2, and $CaCO_3$ were the second most abundantly encountered in subway platform samples, with relative abundances ranging in 6.0-14.0% (Table 1). Some of soil-derived particles were found as internal mixtures of carbonaceous species (denoted as Aluminosilicates/C and SiO_2/C). Soil-derived particles are one of the most abundant aerosol types in ambient urban atmosphere, especially in the coarse fractions, whereby it is expected that those particles came from an outdoor environment. However, it was suggested that some of the Si-, Al-, and S-rich particles in subway aerosol

could come from the wear of paints at subway tunnels, or from construction activities in the tunnels (Sitzmann *et al.*, 1999). If the particles were generated in the indoor subway system, the particles may contain iron species which is ubiquitous in subway indoor environments. Indeed, some of aluminosilicates and $CaCO_3$ particles were found as internal mixture of iron oxide. In this study, they were classified as Fe-containing particles. Considerably less amounts of soil-originated particles in the summertime samples (Table 1) reflect the limited air-exchange between the indoor and outdoor environments.

Nitrate- and Sulfate-containing Particles

They were also significantly encountered in subway aerosol samples, and existed mostly in the chemical forms of Ca(NO_3, SO_4), (Na, Mg) (NO_3, SO_4), and $(NH_4)_2SO_4$. Particles denoted as Ca(NO_3, SO_4) were the internal mixture of $Ca(NO_3)_2$ and $CaSO_4$ and were produced by the atmospheric reaction of $CaCO_3$ with nitrogen and sulfur oxide species (Hwang and Ro, 2006; Ro *et al.*, 2005; Krueger *et al.*, 2004). Similarly, (Na, Mg) (NO_3, SO_4) particles are the mixture of nitrate and sulfate formed by the reaction of sea-salts with nitrogen and sulfur oxide species in the air (Hwang and Ro, 2006; Ro *et al.*, 2005; Laskin *et al.*, 2003). These secondary particles containing nitrates and/or sulfates are likely from the outdoor environment. Since nitrogen and sulfur oxides are abundant gaseous species in the indoor subway microenvironment, such nitrate and sulfate particles can also be formed by the reaction of $CaCO_3$ and sea-salts from the outdoor with indoor gaseous nitrogen and sulfur oxides.

$(NH_4)_2SO_4$ Particles

They are a major chemical species in urban aerosols, especially in fine fractions. In this study, the $(NH_4)_2SO_4$ particles were encountered only at stage 5 ($1\ \mu m < D_p < 2\ \mu m$). Nitrate- and sulfate-containing particles were encountered less frequently in the summer samples (Table 1), mainly due to less air-exchange in the summer and less introduction of outdoor particles into the subway system. Some studies suggested that subway particles are well correlated with the outdoor environment, implying that air-exchange between underground and aboveground environments is well established (Branis, 2006; Aarnio *et al.*, 2005), whereas the others suggested that they are not correlated (Salma *et al.*, 2007; Sitzmann *et al.*, 1999).

4. 4 Arctic Aerosols

4. 4. 1 Introduction

The Arctic atmosphere is regarded as a unique natural laboratory to understand the occurrence, nature, origin, and transport of atmospheric aerosols and their effect on global climate change (Kawamura *et al.*, 2007; Law and Stohl, 2007; Lohmann and Leck, 2005; Yli-Tuomi *et al.*, 2003). It has been observed that atmospheric aerosols were often disturbed by the well-known Arctic haze, a winter/spring Arctic pollution phenomenon (Law and Stohl, 2007; Teinila *et al.*, 2003), suggesting that the atmosphere of the Arctic region could be polluted by anthropogenic air pollutants in the winter and spring. The summertime Arctic atmosphere has been generally regarded as a clean background environment with low aerosol burden and pollution levels. Many research stations from many countries are located in Svalbard, Norway, and Korean Polar Research Center (KPRC) located at Ny-Ålesund (78° 55′N, 11° 56′E), Svalbard is one of them. Svalbard is an archipelago in the Arctic Ocean, including three populated islands: Spitsbergen, Bear Island, and Hopen. Ny-Ålesund is located at the remote northern settlement of Spitsbergen, where the sun is above the horizon for 24 hours a day from late April to late August. To characterize the summertime ambient Arctic aerosol particles, aerosol samples were collected at KRPC and investigated using low-*Z* particle EPMA technique.

4. 4. 2 Sampling and Measurements

16 sets of Arctic aerosol samples were collected at KPRC using a seven-stage May cascade impactor (May, 1975) on July 25-31, 2007. Sampling durations for each stage were adjusted to avoid the collection of agglomerated particles. Individual particles were measured by a JEOL JSM-6390 SEM equipped with an Oxford Link SATW ultra-thin window EDX detector. X-ray spectra were obtained using INCA software (Oxford). Overall, about 8100 individual particles (~150 individual particles on each stage) were manually investigated to obtain information on their size, secondary electron image (SEI), and chemical composition. Samples on stages 1-6 were measured due to the resolution of SEM. Particles on stage 6 were denoted as $PM_{0.5\text{-}1}$, which means the particle diameters were in the range of 0.5-1 μm. In the same way, particles on stages 2-5 were denoted as $PM_{8\text{-}16}$, $PM_{4\text{-}8}$, $PM_{2\text{-}4}$, $PM_{1\text{-}2}$, respectively.

4. 4. 3 Results and Discussion

Based on the X-ray spectra and SEI data of all the analyzed individual particles, 13 particle types were identified. Their characteristics and relative abundances in different stage samples are described below.

Sea-salt Aerosols (SSA)

They are ubiquitous in the marine boundary layer

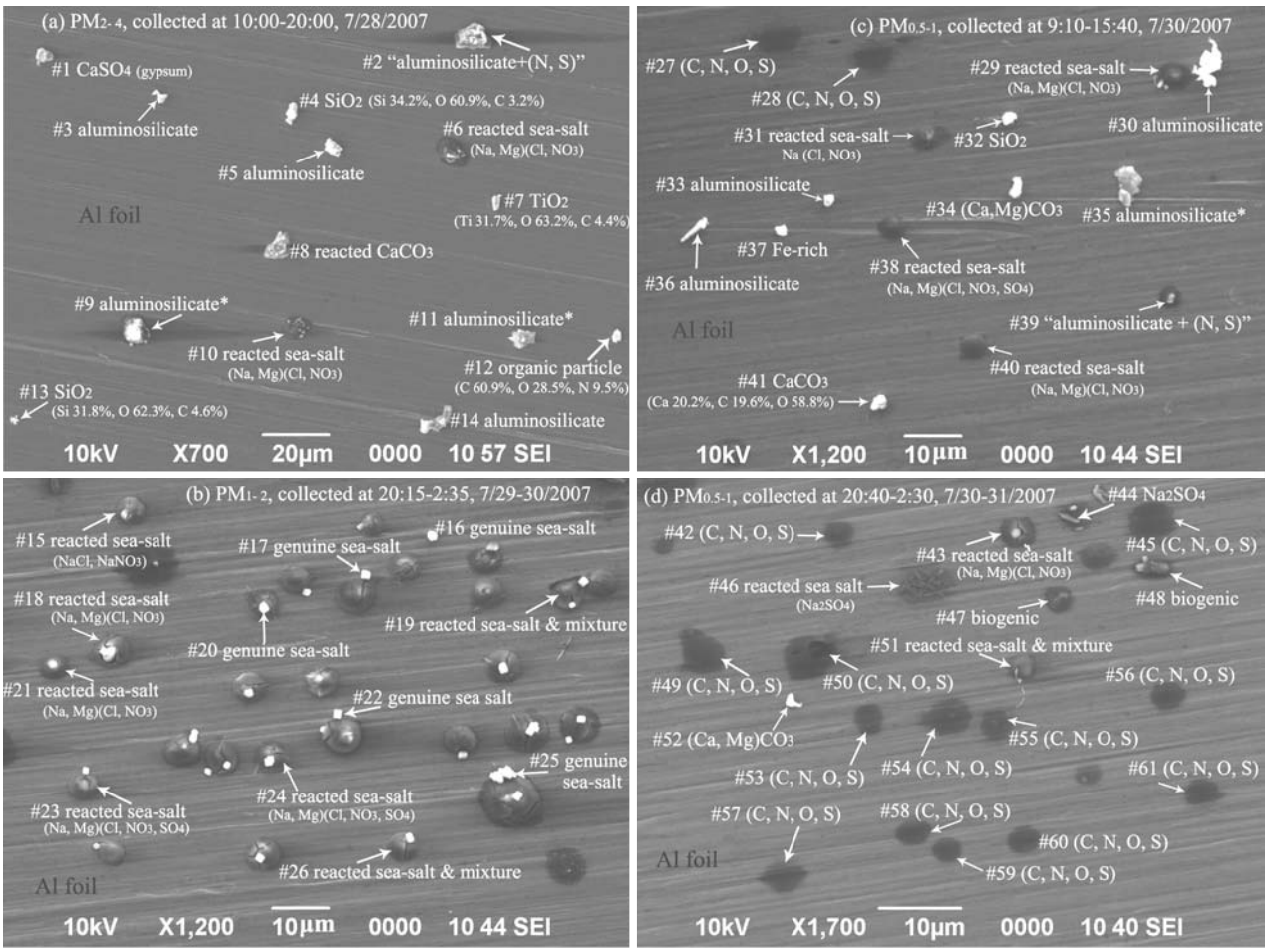

Fig. 12. Typical secondary electron images of aerosol particles collected at Ny-Ålesund, Svalbard. Droplets rich in C, N, O, and S are abbreviated as "(C, N, O, S)", which are likely the mixture of elemental/organic carbon and $H_2SO_4/NH_4HSO_4/(NH_4)_2SO_4$. "Aluminosilicate*" is for aluminosilicate particles containing Fe, for example, particles no. 9, 11, and 35. Reprinted from permission from ref. Geng *et al.*, 2010. Copyright 2010 American Chemical Society.

(MBL) (Athanasopoulou *et al.*, 2008). Shown in Fig. 12 are secondary electron images of Arctic aerosol particles. The size dependency of major particle types was observed, i.e., the frequent observation of soil-derived particles is in coarse fraction (PM_{2-4}) and carbonaceous particles in fine fraction ($PM_{0.5-1}$). Most of sea-salt particles were found in PM_{1-2}. The genuine (or fresh) sea-salt particles were cubic in shape and looked bright on SEI (e.g., particles #16 and #17 in Fig. 12b). In general, genuine sea-salt particles contained small amount of oxygen, which likely came from the NaOH shell, an alkaline hygroscopic coating around the NaCl (Laskin *et al.*, 2003). Occasionally, $MgCO_3$ and $MgSO_4$, which might originate from the evaporation of sea salts, were observed.

In the atmosphere, the reacted (or aged) sea-salts containing $NaNO_3$ and/or Na_2SO_4 are produced when genuine sea-salts react with nitrogen and sulfur oxides species, which results in chlorine loss, sometimes without remaining any chloride if the reaction is complete (Hopkins *et al.*, 2008; Laskin *et al.*, 2002). Hence, SSA often acts as a sink for anthropogenic gases such as nitrogen and sulfur oxides species. In this study, the reacted sea-salts were classified into three types based on their X-ray spectral data. The first type is for those containing nitrates such as Na(Cl, NO_3) and (Na, Mg) (Cl, NO_3), which are the reaction products of genuine sea-salts and NO_x or HNO_3, e.g. particles #6, #10, #15, #18, #21, #29, #31, #40, and #43 in Fig. 12. Particles internally mixed with NaCl, $MgCl_2$, $NaNO_3$, and $Mg(NO_3)_2$ were denoted as (Na, Mg)(Cl, NO_3). The second type is for those containing methanesulfonate ($CH_3SO_3^-$) and non-sea-salt sulfate (nss-SO_4^{2-}) such as Na_2SO_4 and (Na, Mg)SO_4 (e.g., particle

#46 in Fig. 12), which resulted from the reaction of genuine sea-salts with SO_2/H_2SO_4 or methylsulfonic acid (MSA) — a product of dimethylsulfide (DMS) (Hopkins *et al.*, 2008). The third type is for those containing both NO_3^- and $CH_3SO_3^-$/nss- SO_4^{2-}, e.g. particles #23, #24, and #38 in Fig. 12. Sometimes, the reacted sea-salts were found as a mixture with mineral dust particles, which were classified into the "reacted sea-salt & mixture" group, e.g. particles #19, #26, and #51 in Fig. 12.

The majority of reacted sea-salt (& mixture) particles were nitrate-containing. Their round or semispherical shape on SEIs (Fig. 12) indicates that they were liquid droplets at the time of collection. The presence of water greatly enhances the reactivity of NaCl with gaseous materials such as HNO_3, $ClONO_2$, and N_2O_5. If hygroscopic nitrates were formed, due to the low deliquescence and efflorescence points of the secondary SSA particles, they remain as liquid droplet (Hoffman *et al.*, 2004; Laskin *et al.*, 2002). When these liquid droplets were collected on the substrate foil, water started to evaporate and fractionally crystallized particles were formed as illustrated in Fig. 12b. The abundances of nitrate-containing sea-salt particles greatly outweighed those of the $CH_3SO_3^-$ /nss-SO_4^{2-}-containing ones for all the samples except the sample collected on July 27, 2007. Why were such a large number of nitrate-containing sea-salt particles formed and where did NO_x come from in the summertime Arctic region? The possible explanations are described as follows: (1) Sunlight or solar radiation provides favorable conditions for the enhancement of the reaction of NO_x (or HNO_3) and sea-salt aerosols. Gard *et al.* (1998) observed that active heterogeneous chemical reaction of sea-salt particles and NO_x (or HNO_3) primarily occurred during the daytime. It was also reported that sea-salt particles were almost unprocessed during the nighttime, while they were completely converted mostly into $NaNO_3$ particles during the daytime (Laskin *et al.*, 2002). At Ny-Ålesund, the all-day-long daytime during the sampling period should enhance photochemical activities, consequently resulting in the production of nitric acid that readily reacts with sea-salt particles. (2) Levels of NO_x and some precursors of secondary aerosols are increasing in the Arctic Ocean because of the rapid increase of shipping traffic in the region (Xie *et al.*, 2007; Xie *et al.*, 2006). It was reported that the high level of nitrate was observed over and downwind of shipping lanes, as its relatively low deposition rate of high level of NO_x species emitted from travelling ships provided ample time for rate-limited mass transfer for the displacement of chloride (Athanasopoulou *et al.*, 2008). In Russian, Canadian, and U.S. Arctic regions, shipping activities such as the running of icebreakers, transportation of crude oil, and deliveries of general cargo and petroleum products are extensive. Air pollutant emissions from shipping traffic and fuel usage along the main navigation routes in the Arctic Ocean should have an impact on chemical compositions of the Arctic aerosols in the marine boundary layer (Xie *et al.*, 2007; Xie *et al.*, 2006). (3) Anthropogenic air pollutants such as nitrogen and sulfur oxides from industrial emissions in northern Europe and western Siberia can be transported to Ny-Ålesund during the summer (Yli-Tuomi *et al.*, 2003; Ohta *et al.*, 1996). (4) Renoxification (i.e., reduction of NO_3^- to NO_x and HONO) may be one of the most important mechanisms (Morin *et al.*, 2008; Nyeki *et al.*, 2005). During the continuous daytime in the Arctic region, photochemically induced reactions are active. Photochemical reactions occurring within the snowpack or on the snow/ice surface where NO_x and NO_3^- were accumulated or enriched in the winter and spring (particularly when the Arctic haze occurred) can produce high level of NO_x from nitrate (Ianniello *et al.*, 2002). Under solar radiation, the deposited NO_3^- on the Arctic snowpack or ice can be reactivated or reduced to nitrite (NO_2^-) or to NO_2 and hydroxyl radicals (OH), which may eventually lead to reemission of nitrogenous compounds to the atmosphere (Beine *et al.*, 2003), resulting in elevated reacted (aged) sea-salt particles by the reaction of NO_x or HNO_3 with sea salts. The nitrogen cycling rates in the Arctic were reported to increase as shrub growth is stimulated by increasing summer temperature and nitrogen supply (Chapin *et al.*, 2005). Also, the acceleration of summer warming in the Arctic region can result in the advancing of snowmelt and the declining of summer sea ice. (5) The decomposition of peroxyacetyl nitrate (PAN) in the Arctic atmosphere during the polar night period also contributes to the formation of NO_2 (Beine and Krogne, 2000). The thermal decomposition of PAN to NO_2 in the Arctic troposphere (e.g., at Svalbard) occurs mostly in the summer, although the amounts of PAN and NO_2 from PAN are small (Morin *et al.*, 2008).

Mineral Dust Particles

They include aluminosilicate (AlSi-containing), quartz (SiO_2), calcite ($CaCO_3$)/dolomite ($CaMg(CO_3)_2$), gypsum ($CaSO_4 \cdot 2H_2O$), Fe-rich (mostly iron oxides), and rutile (TiO_2). They were popular in coarse fraction and appeared irregular and bright on their SEIs (see Fig. 12a). Fe-rich particles look angular on their SEIs and it is well known that they can act as a nutrient for biota in marine environments with their depositions (Xie *et al.*, 2007). Reacted mineral dust parti-

cles were classified mainly as "reacted $CaCO_3$/CaMg$(CO_3)_2$" and "aluminosilicate+(N, S)" types in which (N, S) notation represented compounds containing either nitrates, sulfates, or both. They are produced when aluminosilicate (especially Ca-containing) and $CaCO_3$/CaMg$(CO_3)_2$ particles react with airborne sulfur and nitrogen oxides in the presence of moisture or with "secondary acids" such as H_2SO_4, HNO_3, and HCl (Sullivan *et al.*, 2007; Hwang and Ro, 2006; Lan *et al.*, 2005). They can be formed either through the reaction of aluminosilicate and $CaCO_3$/CaMg$(CO_3)_2$ particles with H_2SO_4 and/or HNO_3, or from adsorption of NH_4NO_3 or $(NH_4)_2SO_4$/NH_4HSO_4 on particle surface (Sullivan *et al.*, 2007), e.g., particles #2, #8, and #39 in Fig. 12.

Carbonaceous Particles

They are generated mainly from incomplete combustion of fossil fuels and biomass, are ubiquitous in the tropospheric atmosphere, and have strong radiative-forcing effects (Chen *et al.*, 2005). Carbonaceous particles are generally differentiated into two groups: elemental carbon (EC, termed "carbon-rich particle" herein) and organic carbon (OC). In this study, the particle was classified as carbon-rich (or EC) when the carbon content was 3-fold greater than the oxygen content and no other elements were present (Ro *et al.*, 2005). Other carbonaceous particles which have more than 90% atomic concentration of C and O (sometimes including N) were classified as OC.

The OC particles were categorized into four different types based on their morphological and X-ray spectral data. The first type was of primary or water-insoluble secondary organic particles, which look bright and angular on their SEI and have high levels of C, N, and O. It has been termed (C, N, O)-rich particles or nitrogen-containing organic compounds (NOC) by other researchers (Laskin *et al.*, 2009), and may be generated mostly by biomass burning. The second type was of biogenic particles (e.g., pollen, spore, algae, bacteria, and plant or insect fragments), a special type of organic particles. They have a "biogenic fingerprint", i.e., the presence of N, K, P, S and/or Cl together with C and O (e.g. particles #47 and #48 in Fig. 12d) (Geng *et al.*, 2009a, b). Most of the biogenic particles were likely from the seawater of the Arctic Ocean or the surrounding seas nearby the sampling site. The third type was of liquid droplet particles (probably containing water-soluble organic carbon (WSOC)), which looked dark with round shape and had high levels of C, N, and O, often together with a trace amount of Na and Mg elements indicating their marine origin. These (C, N, O)-rich droplets were possibly composed of organic matter and NH_4NO_3. Oxidation of volatile organic compounds, humic substances or "humic-like substances (HULIS)" in the marine environment, and crude oils spilled on the sea surface from ship tankers are perhaps contributory to the organic matter (Geng *et al.*, 2009b). The fourth type of OC particles was of droplet particles rich in C, N, O, and S, represented as (C, N, O, S)-rich droplets, which were also significantly observed in the summertime aerosol samples collected at Tokchok Island, Korea (Geng *et al.*, 2009a). They look dark on their SEIs (e.g., many particles in Fig. 12d) and are likely internally mixed with $(NH_4)_2SO_4$/NH_4HSO_4 and organic matter. Ambient sulfate is often neutralized by ammonia (mainly from animal waste, fertilizer application, soil and industrial emissions, and direct emissions from vegetation and oceans) and its most common form is $(NH_4)_2SO_4$. However, if ammonia is scarce, sulfate can remain in more acidic forms such as NH_4HSO_4 or H_2SO_4 (Ansari *et al.*, 1998). Ammonia is usually scarce in the Arctic region being without major ammonia sources (Teinila *et al.*, 2003), so that the (C, N, O, S)-rich droplet particles might include more acidic NH_4HSO_4 (or H_2SO_4) rather than $(NH_4)_2SO_4$. There are three possible sources of SO_2 and SO_4^{2-} in the Arctic region: the first is from ship emissions around the Arctic Ocean (Xie *et al.*, 2007, 2006); the second is likely from industrial emissions in western Siberia (Russia) and northern Europe; the third is from DMS in seawater, as high biological activity in ocean margins results in a significant production of DMS, which can be oxidized to form various sulfur containing products, such as MSA, SO_2, nss-SO_4^{2-} (Yang *et al.*, 2009; Hopkins *et al.*, 2008). The organic matter in the (C, N, O, S)-rich droplet particles is likely similar to that in the (C, N, O)-rich droplets. Perhaps, some products of DMS are involved (Hopkins *et al.*, 2008).

Soot agglomerates, which are abundant in urban atmosphere, were not observed in the summertime Arctic samples, possibly due to the absence of combustion sources of diesel oil or coal in Ny-Ålesund. A few tar balls and chars were observed, which have irregular or spherical morphology, quite different from that of soot aggregates. They can be generated by gas-to-particle conversion within smoke plumes and are particularly abundant in slightly aged biomass smoke (Pósfai *et al.*, 2004).

Relative Abundances of Various Types of Particles

The relative abundances of particle types observed in 16 summertime Arctic samples are shown in Fig. 13. Arctic aerosols were classified into three groups according to their origins: marine-originated, soil-derived, and carbonaceous. Marine-originated particles

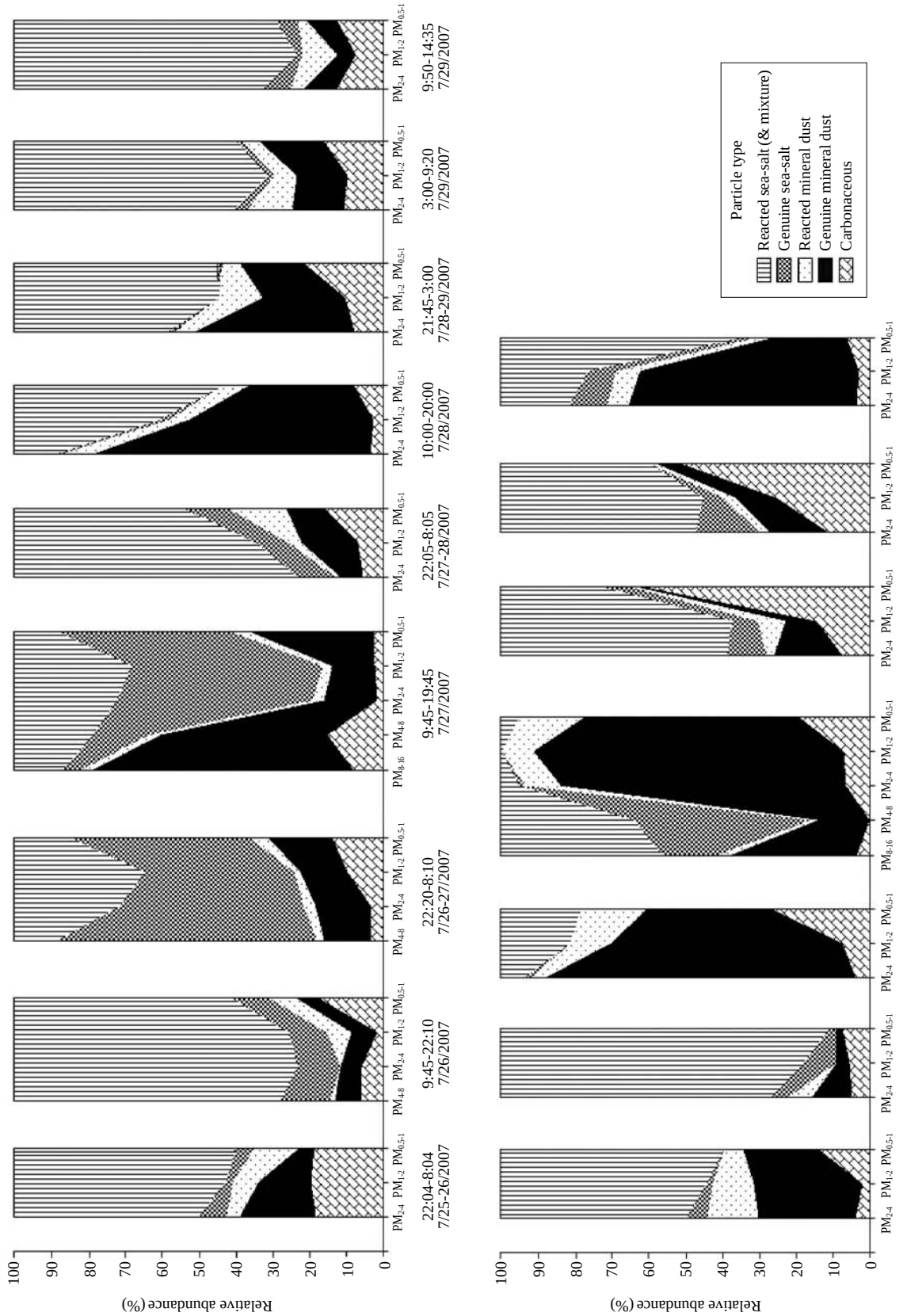

Fig. 13. Relative abundances of various particle types in summertime Arctic samples. Reprinted from permission from ref. Geng *et al.*, 2010. Copyright 2010 American Chemical Society.

contain genuine and aged (reacted) sea-salt particles. The aged sea-salts including nitrates and/or sulfates were produced by the reaction between sea-salts and NO_x/SO_x. In Arctic aerosol samples, sea-salt particles were the most frequently encountered with more than 50% relative abundance, and most of them were observed as aged (reacted) species. However, the relative abundances of reacted sea-salt depended on the passage of air mass. Similar observation was reported by Friedman *et al.* (2009).

Soil-originated mineral dust particles contained aluminosilicate, $CaCO_3/(Ca,Mg)CO_3$, SiO_2, $CaSO_4$, and Fe-rich particles, among which aluminosilicate particles were the most frequently encountered. The relative abundances of mineral dust particles (including reacted ones) were in the range of 25-35% and they were observed mainly in coarse fraction (PM_{8-16} and PM_{4-8}). The non-reacted mineral dust particles outnumbered the reacted ones (only 5.3%, 6.4%, and 7.0% on average for PM_{4-2}, PM_{2-1}, and $PM_{1-0.5}$ fractions, respectively). Many of the mineral dust particles should be of local origin, mostly from snow-free mountains during summertime (Teinila *et al.,* 2003). The possible reasons for the predominance of the genuine mineral dust particles over the reacted ones are: (i) anthropogenic emissions were not strong in the remote Arctic region so that mineral dust particles had no chance to react with air pollutants; (ii) the reactivity of mineral dust particles with NO_x and SO_2 was much slower than that of sea-salts (Kang *et al.*, 2009). Like the reacted sea-salt particles, the reacted mineral dust particles containing nitrates were predominant over those containing sulfates, indicating that NO_x or HNO_3 contributed to the formation of reacted mineral dust particles more than SO_2 or H_2SO_4 did.

Most of organic carbon (OC) particles were primarily composed of liquid droplets rich in (C, N, O) and (C, N, O, S), and it was hard to find carbon-rich ones. It implies that the summertime Arctic atmosphere was more affected from the mixture of organic matter and secondary anthropogenic pollutants such as NH_4NO_3 and $NH_4HSO_4/(NH_4)_2SO_4$ than EC particles, which are produced from smoke plumes of forest fires or from oil combustion by ships around the periphery of the Arctic Ocean (Xie *et al.*, 2007). The relative abundances of (C, N, O, S)-rich droplets were much higher than those of (C, N, O)-rich droplets. On average, (C, N, O)-rich droplets were encountered with relative abundances of 1.9%, 1.7%, and 3.4% in PM_{4-2}, PM_{2-1}, and $PM_{1-0.5}$ fractions, respectively; whereas (C, N, O, S)-rich droplets were significantly encountered in PM_{4-2}, PM_{2-1}, and $PM_{1-0.5}$ fractions for almost all the samples, peaking at 50-60% of relative abundances for PM_{4-2} fraction of samples collected at 20:40-8:40, 7/30-31/2007. Possible reasons for this observation are (i) $NH_4HSO_4/(NH_4)_2SO_4$ was easier to be formed in the summer than NH_4NO_3 and/or (ii) the air masses that originated from continental European countries and passed over the south Arctic Ocean and Barents Sea carried more NH_3 and SO_2. It has been reported that air masses from western Siberia can be contaminated by anthropogenic pollutants such as SO_2 from smelting factory in Norilsk (Ohta *et al.*, 1995). And nss-sulfate concentrations in precipitations at Ny-Ålesund were reported to be high when air masses had passed over Scandinavia and western Siberia regions (Yamagata *et al.*, 2009).

5. Summary

In this review, the development and methodology of low-*Z* particle EPMA for the analysis of atmospheric aerosols are introduced and the characteristic physicochemical properties and origins of various atmospheric aerosol particles, such as Asian dust, urban aerosols, subway particles, and Arctic aerosols are described. Low-*Z* particle EPMA technique is capable of the quantitative determination of low-*Z* elements in microscopic volume by utilizing a methodology of automated Monte Carlo calculations in an iterative approach. The ability of analyzing low-*Z* elements in microscopic volume enlarges the applicability of this technique for the analysis of atmospheric aerosol particles. Furthermore, the diversity and the complicated heterogeneity of atmospheric aerosol particles can be investigated in detail.

The major chemical species found in the Asian Dust particles collected during Asian Dust phenomena in Korea were aluminosilicate, silicon dioxide, calcium-containing, marine-originated, and carbonaceous particles. Overall, the soil-derived particles such as aluminosilicate, silicon dioxide, and calcium-containing particles were the most common. However, the relative abundances of those particles on the basis of their size were different case by case. Some samples contained relatively large fraction of sea-salt related particles, either genuine or reacted sea-salts, entrained during their passage through the Yellow Sea. For some samples, the considerable amount of nitrate and/or sulfate particles were encountered, implying that $CaCO_3$ and sea-salts particles had reacted with SO_x/NO_x species during their long-range transport. It shows that the chemical composition and the relative abundances of the chemical species of Asian Dust particles depend on the pathway and the moving speed of the air-mass, and the meteorological conditions.

Urban aerosols collected in three cities (Seoul as a

megacity; CheongJu as a relatively small city with industrial complexes; ChunCheon as a city of low population without industrial complexes) of Korea, having different urban characteristics in terms of their population, size, and industrial circumstances, were investigated. In general, carbonaceous, aluminosilicates, silicon dioxide, and calcium carbonate aerosol particles were major components in urban atmospheric particles. In Seoul sample, soil-originated and carbonaceous particles were most abundant in the coarse and fine fractions, respectively. However, in CheongJu sample, ammonium sulfate particles were most abundant in the fine fraction. In addition, calcium sulfate and nitrate particles, presumably the product of a reaction between soil-derived $CaCO_3$ species and anthropogenic SO_x/NO_x, were significantly observed. In ChunCheon sample, organic particles were most abundant in the fine fraction and sodium nitrate particles were seen at high levels, which seemed to be influenced by sea-salts aerosols originating from the Yellow Sea.

Subway particles, collected in Hyehwa underground subway station in Seoul, Korea, were investigated. Four major types of subway particles, based on their chemical compositions, were significantly encountered: Fe-containing; soil-derived; carbonaceous; and secondary nitrate and/or sulfate particles. Fe-containing particles were generated from wear processes at rail-wheel-brake interfaces while the others were mostly introduced from the outdoor urban atmosphere. Fe-containing particles were the most frequently encountered with relative abundances in the range of 61-79%, and existed either as partially or fully oxidized forms. Relative abundances of Fe-containing particles increased as particle size decreased. There was a seasonal difference in the composition of subway particles such that the summertime samples contained the most abundant Fe-containing particles, whereas soil-derived and nitrate/sulfate particles were the least, indicating the limited air-exchange between indoor and outdoor environments owing to the air-conditioning in the subway system.

Summertime Arctic aerosols, collected at Ny-Ålesund, Svalbard, Norway, most abundantly contained marine originated particles, followed by carbonaceous and mineral dust particles. A number of aged (reacted) sea salt (& mixture) particles produced by the atmospheric reaction of genuine sea-salts, especially with NO_x (or HNO_3), were significantly encountered in almost all the Arctic aerosol samples. They greatly outnumbered genuine sea salt particles, implying that the summertime Arctic atmosphere, generally regarded as a clean background environment, is disturbed by anthropogenic air pollutants. The main sources of airborne NO_x (or HNO_3) are probably ship emissions around the Arctic Ocean, industry emission from northern Europe and northwestern Siberia, and renoxification of NO_3^- within or on the melting snow/ice surface.

ACKNOWLEDGEMENTS

This work was supported by the Korea Research Foundation Grant funded by the Korean Government (MOEHRD, Basic Research Promotion Fund) (KRF-2006-311-D00600).

REFERENCES

Aarnio, P., Yli-Tuomi, T., Kousa, A., Makela, T., Hirsikko, A., Hameri, K., Raisanen, M., Hillamo, R., Koskentalo, T., Jantunen, M. (2005) The concentrations and composition of and exposure to fine particles ($PM_{2.5}$) in the Helsinki subway system. Atmospheric Environment 39, 5059-5066.

Adams, H.S., Nieuwenhuijsen, M.J., Colvile, R.N. (2001a) Determinants of fine particle ($PM_{2.5}$) personal exposure levels in transport microenvironments, London, UK. Atmospheric Environment 35, 4557-4566.

Adams, H.S., Nieuwenhuijsen, M.J., Colvile, R.N., McMullen, M.A.S., Khandelwal, P. (2001b) Fine particle ($PM_{2.5}$) personal exposure levels in transport microenvironments, London, UK. Science of the Total Environment 279, 29-44.

Ansari, A.S., Pandis, S.N. (1998) Response of inorganic PM to precursor concentrations. Environmental Science and Technology 32, 2706-2714.

Armstrong, J.T., Buseck, P.R. (1985) A general characteristic fluorescence correction for the quantitative electron microbeam analysis of thick specimens, thin films and particles. X-Ray Spectrometry 14, 172-182.

Armstrong, J.T. (1991) Electron Probe Quantitation (Heinrich K.F.J. and Newbury, D.E. Eds.), Plenum Press, New York, pp. 261-316.

Athanasopoulou, E., Tombrou, M., Pandis, S.N., Russell, A.G. (2008) The role of sea-salt emissions and heterogeneous chemistry in the air quality of polluted coastal areas. Atmospheric Chemistry and Physics 8, 3807-3841.

Beine, H.J., Krognes, T. (2000) The seasonal cycle of peroxyacetyl nitrate (PAN) in the European Arctic. Atmospheric Environment 34, 933-940.

Beine, H.J., Domine, F., Ianniello, A., Nardino, M., Allegrini, I., Teinila, K., Hillamo, R. (2003) Fluxes of nitrates between snow surfaces and the atmosphere in the European high Arctic. Atmospheric Chemistry and Physics 3, 335-346.

Birenzvige, A., Eversole, J., Seaver, M., Francesconi, S, Valdes, E., Kulaga, H. (2003) Aerosol Characteristics in a Subway Environment. Aerosol Science Techno-

logy 37, 210-220.
Bishop, A.N., Kearsley, A.T., Patience, R.L. (1992) Analysis of sedimentary organic materials by scanning electron microscopy: the application of backscattered electron imagery and light element X-ray microanalysis. Organic Geochemistry 18, 431-446.
Branis, M. (2006) The contribution of ambient sources to particulate pollution in spaces and trains of the Prague underground transport system. Atmospheric Environment 40, 348-356.
Carmichael, G.R., Hong, M., Ueda, H., Chen, L., Murano, K., Park, J.K., Lee, H., Kim, Y., Shim, S. (1997) Aerosol Composition at Cheju Island, Korea. Journal of Geophysical Research D5, 6047-6061.
Carson, P.G., Johnston, M.V., Wexler, A.S. (1997) Real-Time Monitoring of the Surface and Total Composition of Aerosol Particles. Aerosol Science and Technology 26, 291-300.
Chapin, III, F.S., Sturm, M., Serreze, M.C., McFadden, J.P., Key, J.R., Lloyd, A.H., McGuire, A.D., Rupp, T.S., Lynch, A.H., Schimel, J.P., Beringer, J., Chapman, W.L., Epstein, H.E., Euskirchen, E.S., Hinzman, L.D., Jia, G., Ping, C.-L., Tape, K.D., Thompson, C.D.C., Walker, D.A., Welker J.M. (2005) Role of land-surface changes in arctic summer warming. Science 310, 657-660.
Chen, Y., Shah, N., Braun, A., Huggins, F.E., Huffman, G.P. (2005) Electron microscopy investigation of carbonaceous particulate matter generated by combustion of fossil fuels. Energy Fuels 19, 1644-1651.
Chillrud, S.N., Epstein, D., Ross, J.M., Sax, S.N., Pederson, D., Spengler, J.D., Kinney, P.L. (2004) Elevated Airborne Exposures of Teenagers to Manganese, Chromium, and Iron from Steel Dust and New York City's Subway System. Environmental Science and Technology 36, 732-737.
Chow, J.C., Liu, C.S., Cassmassi, J., Watson, J.G., Lu, Z., Pritchett, L.C. (1992) A neighborhood-scale study of PM_{10}. Atmospheric Environment 26A, 693-706.
Dentener, F.J., Carmichael, G.R., Zhang, Y., Lelieveld, J., Crutzen, P.J. (1996) Role of mineral aerosol as a reactive surface in the global troposphere. Journal of Geophysical Research D17, 22869-22889.
Drouin, D., Hovington, P., Gauvin, R. (1997) CASINO: A New Monte Carlo Code in C Language for Electron Beam Interactions-Part II: Tabulated Values of the Mott Cross Section. Scanning 19, 20-28.
Friedman, B., Herich, H., Kammermann, L., Gross, D.S., Arneth, A., Holst, T., Cziczo, D.J. (2009) Subarctic atmospheric aerosol composition: 1. Ambient aerosol characterization. Journal of Geophysical Research 114, D13203, doi:10.1029/2009JD011772.
Frustorfer, P., Niessner, R. (1994) Identification and Classification of Airborne soot Particles Using an Automated SEM/EDX. Mikrochimica Acta 113, 239-250.
Furuya, K., Kudo, Y., Okinaga, K., Yamuki, M., Takahashi, S., Araki, Y., Hisamatsu, Y. (2001) Seasonal variation and their characterization of suspended particulate matter in the air of subway stations. Journal of Trace and Microprobe Techniques 19, 469-485.
Gard, E., Mayer, J.E., Morrical, B.D., Dienes, T., Fergenson, D.P., Prather, K.A. (1997) Real-Time Analysis of Individual Atmospheric Aerosol Particles: Design and Performance of a Portable ATOFMS. Analytical Chemistry 69, 4083-4091.
Gard, E.E., Kleeman, M.J., Gross, D.S., Hughes, L.S., Allen, J.O., Morrical, B.D., Fergenson, D.P., Dienes, T., Gälli, M.E., Johnson, R.J., Cass, G.R., Prather, K.A. (1998) Direct observation of heterogeneous chemistry in the atmosphere. Science 279, 1184-1187.
Geng, H., Jung, H.-J., Park, Y., Hwang, H., Kim, H., Kim, Y.J., Sunwoo, Y., Ro, C.-U. (2009a) Morphological and chemical composition characteristics of summertime atmospheric particles collected at Tokchok Island, Korea. Atmospheric Environment 43, 3364-3373.
Geng, H., Park, Y., Hwang, H., Kang, S., Ro, C.-U. (2009b) Elevated nitrogen-containing particles observed in Asian dust aerosol samples collected at the marine boundary layer of the Bohai Sea and the Yellow Sea. Atmospheric Chemistry and Physics 9, 6933-6947.
Geng, H., Ryu, J., Jung, H.-J., Chung, H., Ahn, K., Ro, C.-U. (2010) Single-Particle Characterization of Summertime Arctic Aerosols Collected at Ny-Alesund, Svalbard, Environmental Science and Technology 44, 2348-2353.
Goldstein, J.I., Newbury, D.E., Joy, D.C., Lyman, C., Echlin, P., Lifshin, E., Sawyer, L., Michael, J. (2003) Scanning Electron Microscopy and X-ray Microanalysis (3rd Ed.) Kluwer-Plenum, New York, pp. 391-450.
Hamilton, R.S., Kershaw, P.R., Segarra, F., Spears C.J., Watt, J.M. (1994) Detection of airborne carbonaceous particulate matter by scanning electron microscopy. Science of the Total Environment 146/147, 303-308.
Harrington, P.B., Street, T.E., Voorhees, K.J., di Brozolo, F.R., Odom, R.W. (1989) Rule-Building Expert System for Classification of Mass Spectra. Analytical Chemistry 61, 715-719.
Hoffman, R.C., Laskin A., Finlayson-Pitts, B.J. (2004) Sodium nitrate particles: physical and chemical properties during hydration and dehydration, and implications for aged sea salt aerosols. Journal of Aerosol Science 35, 869-887.
Hopkins, R.J., Desyaterik, Y., Tivanski, A.V., Zaveri, R.A., Berkowitz, C.M., Tyliszczak, T., Gilles, M.K., Laskin, A. (2008) Chemical speciation of sulfur in marine cloud droplets and particles: Analysis of individual particles from the marine boundary layer over the California current. Journal of Geophysical Research 113, D04209, doi:10.1029/2007JD008954.
Hovington, P., Drouin, D., Gauvin, R. (1997a) CASINO: A New Monte Carlo Code in C Language for Electron Beam Interactions-Part I: Description of the Program. Scanning 19, 1-14.
Hovington, P., Drouin, D., Gauvin, R., Joy, D.C., Evans, N. (1997b) CASINO: A New Monte Carlo Code in C

Language for Electron Beam Interactions-Part III: Stopping Power at Low Energies. Scanning 19, 29-35.
Hughes, L.S., Allen, J.O., Kleeman, M.J., Johnson, R.J., Cass, G.R., Gross, D.S., Gard, E.E., Gälli, M.E., Morrical, B.D., Fergenson, D.P., Dienes, T., Noble, C.A., Liu, D.Y., Silva, P.J., Prather, K.A. (1999) Size and Composition Distribution of Atmospheric Particles in Southern California. Environmental Science and Technology 33, 3506-3515.
Hwang, H., Ro, C.-U. (2006) Direct observation of nitrate and sulfate formations from mineral dust and sea-salts using low-*Z* particle electron probe X-ray microanalysis. Atmospheric Environment 40, 3869-3880.
Ianniello, A., Beine, H.J., Sparapani, R., Di Bari, F., Allegrini, I., Fuentes, J.D. (2002) Denuder measurements of gas and aerosol species above Arctic snow surfaces at Alert 2000. Atmospheric Environment 36, 5299-5309.
Jambers, W., Van Grieken, R. (1997) Single Particle Characterization of Inorganic Suspension in Lake Baikal, Siberia. Environmental Science and Technology 31, 1525-1533.
Johansson, C., Johansson, P.-A. (2003) Particulate matter in the underground of Stockholm. Atmospheric Environment 37, 3-9.
Karlsson, H.L., Nilsson, L., Moller, L. (2005) Subway Particles Are More Genotoxic than Street Particles and Induce Oxidative Stress in Cultured Human Lung Cells. Chemical Research and Toxicology 18, 19-23.
Karlsson, H.L., Ljungman, A.G., Lindbom, J., Moller, L. (2006) Comparison of genotoxic and inflammatory effects of particles generated by wood combustion, a road simulator and collected from street and subway. Toxicological Letter, 165, 203-211.
Kang, S., Hwang, H., Park, Y., Kim, H., Ro, C.-U. (2008) Chemical compositions of subway particle in Seoul, Korea determined by a quantitative single particle analysis. Environmental Science and Technology 42, 9051-9057.
Kang, S., Hwang, H., Kang, S., Park, Y., Kim, H., Ro, C.-U. (2009) Quantitative ED-EPMA combined with morphological information for the characterization of individual aerosol particles collected in Incheon, Korea. Atmospheric Environment 43, 3445-3453.
Kawamura, K., Narukawa, M., Li, S.-M., Barrie, L.A. (2007) Size distributions of dicarboxylic acids and inorganic ions in atmospheric aerosols collected during polar sunrise in the Canadian high Arctic. Journal of Geophysical Research 112, D10307, doi:10.1029/2006 JD008244.
Koutny, L.B., Yeung, E.S. (1993) Expert System for Data Acquisition To Achieve a Constant Signal-to-Noise Ratio: Application to Imaging of DNA Sequencing Gels. Analytical Chemistry 65, 148-152.
Krueger, B.J., Grassian, V.H., Cowin, J.P., Laskin, A. (2004) Heterogeneous chemistry of individual mineral dust particles from different dust source regions: the importance of particle mineralogy. Atmospheric Environment 38, 6253-6261.
Laskin, A., Iedema, M.J., Cowin, J.P. (2002) Quantitative time-resolved monitoring of nitrate formation in sea salt particles using a CCSEM/EDX single particle analysis. Environmental Science and Technology 36, 4948-4955.
Laskin, A., Gaspar, D.J., Wang, W., Hunt, S.W., Cowin, J.P., Colson, S.D., Finlayson-Pitts, B.J. (2003) Reactions at interfaces as a source of sulfate formation in sea-salt particles. Science 301, 340-344.
Laskin, A., Smith, J., Laskin, J. (2009) Molecular characterization of nitrogen-containing organic compounds in biomass burning aerosols using high-resolution mass spectrometry. Environmental Science and Technology 43, 3764-3771.
Lábár, J.L., Török, S. (1992) A Peak-to-Background Method for Electron Probe X-Ray Microanalysis Applied to Individual Small Particles. X-Ray Spectrometry 21, 183-190.
Law, K.S., Stohl, A. (2007) Arctic Air Pollution: Origins and Impacts. Science 315, 1537-1540.
Lohmann, U., Leck, C. (2005) Importance of submicron surface-active organic aerosols for pristine Arctic clouds. Tellus 57B, 261-268.
May, K.R. (1975) An ultimate cascade impactor for aerosol assessment. Journal of Aerosol Science 6, 1-7.
Morin, S., Savarino, J., Frey, M.M., Yan, N., Bekki, S., Bottenheim, J.W., Martins, J.M. (2008) Tracing the origin and fate of NO_x in the Arctic atmosphere using stable isotopes in nitrate. Science 322, 730-732.
Murphy, D.M., Thomson, D.S. (1997a) Chemical composition of single aerosol particles at Idaho Hill: Positive ion measurements. Journal of Geophysical Research 102, 6341-6352.
Murphy, D.M., Thomson, D.S. (1997b) Chemical composition of single aerosol particles at Idaho Hill: Negative ion measurements. Journal of Geophysical Research 102, 6353-6368.
Noble, C.A., Prather, K.A. (1996) Real-Time Measurement of Correlated Size and Composition Profiles of Individual Atmospheric Aerosol Particles. Environmental Science and Technology 30, 2667-2680.
Nyeki, S., Coulson, G., Colbeck, I., Eleftheriadis, K., Baltensperger, U., Beine, H.J. (2005) Overview of aerosol microphysics at Arctic sunrise: measurements during the NICE renoxification study. Tellus 57B, 40-50.
Ohta, S., Fukasawa, T., Muroa, N., Makarov, V.N. (1995) Summer concentrations of atmospheric pollutants in urban and rural areas of Siberia. Journal of Global Environmental Engineering 1, 15-26.
Osán, J., Török, S., Török, K., Németh, L., Lábár, J.L. (1996) Physiological effect of accidental fly ash deposition on plants and chemical study of the dusted plant leaves by XRF and EPMA. X-ray Spectrometry 25, 167-172.
Osán, J., Szaloki, I., Ro, C.-U., Van Grieken, R. (2000) Light Element Analysis of Individual Microparticles Using Thin-Window EPMA. Mikrochimica Acta 132,

349-355.
Polissar, A.V., Hopke, P.K., Piorot, R.L. (2001) Atmospheric Aerosol over Vermont: Chemical Composition and Sources. Environmental Science and Technology 35, 4604-4621.
Pósfai, M., Gelencsér, A., Simonics, R., Arató, K., Li, J., Hobbs, P.V., Buseck, P.R. (2004) Atmospheric tar balls: Particles from biomass and biofuel burning. Journal of Geophysical Research 109, D06213, doi:10.1029/2003JD004169.
Ro, C.-U., Osán, J., Van Grieken, R. (1999) Determination of low-*Z* elements in individual environmental particles using windowless EPMA. Analytical Chemistry 71, 1521-1528.
Ro, C.-U., Osán, J., Szalóki, I., Oh, K.-Y., Van Grieken, R. (2000) Determination of chemical species in individual aerosol particles using ultrathin window EPMA. Environmental Science and Technology 34, 3023-3030.
Ro, C.-U., Oh, K.-Y., Kim, H., Chun, Y.-S., Osán, J., de Hoog, J., Van Grieken, R. (2001a) Chemical speciation of individual atmospheric particles using low-*Z* electron probe X-ray microanalysis: characterizing "Asian Dust" deposited with rainwater in Seoul, Korea. Atmospheric Environment 35, 4995-5005.
Ro, C.-U., Oh, K.-Y., Kim, H., Kim, Y.P., Lee, C.B., Kim, K.H., Osán, J., de Hoog, J., Worobiec, A., Van Grieken, R. (2001b) Single Particle Analysis of Aerosols at Cheju Island, Korea, Using Low-*Z* Electron Probe X-ray Microanalysis: A Direct Proof of Nitrate Formation from Sea-Salts. Environmental Science and Technology 35, 4487-4494.
Ro, C.-U., Kim, H., Oh, K.-Y., Yea, S.K., Lee, C.B., Jang, M., Van Grieken, R. (2002) Single-Particle Characterization of Urban Aerosol Particles Collected in Three Korean Cities Using Low-*Z* Electron Probe X-ray Microanalysis. Environmental Science and Technology, 36, 4770-4776.
Ro, C.-U., Osán, J., Szalóki, I., de Hoog, J., Worobiec, A., Van Grieken, R. (2003) A Monte Carlo program for quantitative electron-induced X-ray analysis of individual particles. Analytical Chemistry 75, 851-859.
Ro, C.-U., Kim, H., Van Grieken, R. (2004) An Expert System for Chemical Speciation of Individual Particles Using Low-Z Particle Electron Probe X-ray Microanalysis Data. Analytical Chemistry 76, 1322-1327.
Ro, C.-U., Hwang, H., Kim, H., Chun, Y., Van Grieken, R. (2005) Single-Particle Characterization of Four Asian Dust Samples Collected in Korea, Using Low-*Z* Particle Electron Probe X-ray Microanalysis. Environmental Science and Technology 39, 1409-1419.
Salma, I., Weidinger, T., Maenhaut, W. (2007) Time-resolved mass concentration, composition and sources of aerosol particles in a metropolitan underground railway station. Atmospheric Environment 41, 8391-8405.
Satheesh, S.K., Moorthy, K.K. (2005) Radiative effects of natural aerosols: A review, Atmospheric Environment 39, 2089-2110.
Seaton, A., Cherrie, J., Dennekamp, M., Donaldson, K., Hurley, J.F., Tran, C.L. (2005) The London Underground: dust and hazards to health. Occupational and Environmental Medicine 62, 355-362.
Sitzmann, B., Kendal, M., Williams, I. (1999) Characterisation of airborne particles in London by computer-controlled scanning electron microscopy. Science of the Total Environment 241, 63-73.
Sullivan, R.C., Guazzotti, S.A., Sodeman, D.A., Tang, Y., Carmichael, G.R., Prather, K.A. (2007) Mineral dust is a sink for chlorine in the marine boundary layer. Atmospheric Environment 41, 7166-7179.
Szalóki, I., Osán, J., Ro, C.-U., Van Grieken, R. (2000) Quantitative characterization of individual aerosol particles by thin-window EPMA combined with iterative simulation. Spectrochimica Acta B55, 1017-1030.
Teinila, K., Hillamo, R., Kerminen, V.-M., Beine, H.J. (2003) Aerosol chemistry during the NICE dark and light campaigns. Atmospheric Environment 37, 563-575.
Van Borm, W.A., Adams, F.C. (1989) Characterization of individual particles in the Antwerp aerosol. Atmospheric Environment 23, 1139-1151.
Van Borm, W., Adams, F.C., Maenhaut, W. (1990) Receptor modeling of the Antwerp aerosol. Atmospheric Environment 24B, 419-435.
Vekemans, B., Janssens, K., Vincze, L., Adams, F., Van Espen, P. (1994) Analysis of X-ray spectra by iterative least squares (AXIL): new developments. X-Ray Spectrometry 23, 278-285.
Weast, R.C., Astle, M.J., Beyer, W.H., Eds. (1984) CRC Handbook of Chemistry and Physics, CRC Press, Boca Raton, FL, pF-154.
Xie, Z., Sun, L., Blum, J.D., Huang, Y., He, W. (2006) Summertime aerosol chemical components in the marine boundary layer of the Arctic Ocean. Journal of Geophysical Research 111, D10309, doi:10.1029/2005JD006253.
Xie, Z., Blum, J.D., Utsunomiya, S., Ewing, R.C., Wang, X., Sun, L. (2007) Summertime carbonaceous aerosols collected in the marine boundary layer of the Arctic Ocean. Journal of Geophysical Research 112, D02306, doi:10.1029/2006JD007247.
Yamagata, S., Kobayashi, D., Ohta, S., Murao, N., Shiobara, M., Wada, M., Yabuki, M., Konishi, H., Yamanouchi, T. (2009) Properties of aerosols and their wet deposition in the arctic spring during ASTAR2004 at Ny-Ålesund, Svalbard. Atmospheric Chemistry and Physics 9, 261-270.
Yang, G.P., Zhang, H.H., Su, L.P., Zhou, L.M. (2009) Biogenic emission of dimethylsulfide (DMS) from the North Yellow Sea, China and its contribution to sulfate in aerosol during summer. Atmospheric Environment 43, 2196-2203.
Yli-Tuomi, T., Venditte, L., Hopke, P.K., Basunia, M.S., Landsberger, S., Viisanen, Y., Paatero, J. (2003) Composition of the Finnish Arctic aerosol: collection and

analysis of historic filter samples. Atmospheric Environment 37, 2355-2364.

Zhang, D., Shi, G.Y., Iwasaka, Y., Hu, M. (2000) Mixture of sulfate and nitrate in coastal atmospheric aerosols: individual particle studies in Qingdao (36˚04′N, 120˚21′E), China. Atmospheric Environment 34, 2669-2679.

Zhang, W., Chait, B.T. (2000) ProFound: An Expert System for Protein Identification Using Mass Spectrometric Peptide Mapping Information. Analytical Chemistry 72, 2482-2489.

Zhang, Z., Friedlander, S.K. (2000) A Comparative Study of Chemical Databases for Fine Particle Chinese Aerosols. Environmental Science and Technology 34, 4687-4694.

Zimmer, A.T., Biswas, P. (2001) Characterization of the aerosols resulting from arc welding processes. Journal of Aerosol Science 32, 993-1008.

(Received 29 September 2010, accepted 12 November 2010)